


2015

EXTRACTION OF PICTORIAL ENERGY INFORMATION FROM CAMPUS UNMETERED BUILDINGS USING IMAGE PROCESSING TECHNIQUES

Yachen Tang
Michigan Technological University


Follow this and additional works at: <https://digitalcommons.mtu.edu/etds>

 Part of the [Computer Engineering Commons](#), and the [Electrical and Computer Engineering Commons](#)
Copyright 2015 Yachen Tang

Recommended Citation

Tang, Yachen, "EXTRACTION OF PICTORIAL ENERGY INFORMATION FROM CAMPUS UNMETERED BUILDINGS USING IMAGE PROCESSING TECHNIQUES", Master's Thesis, Michigan Technological University, 2015.
<https://digitalcommons.mtu.edu/etds/905>

Follow this and additional works at: <https://digitalcommons.mtu.edu/etds>

 Part of the [Computer Engineering Commons](#), and the [Electrical and Computer Engineering Commons](#)

EXTRACTION OF PICTORIAL ENERGY INFORMATION FROM CAMPUS
UNMETERED BUILDINGS USING IMAGE PROCESSING TECHNIQUES

By

Yachen Tang

A THESIS

Submitted in partial fulfillment of the requirements for the degree of

MASTER OF SCIENCE

In Computer Engineering

MICHIGAN TECHNOLOGICAL UNIVERSITY

2015

© 2015 Yachen Tang

This thesis has been approved in partial fulfillment of the requirements for the Degree of MASTER OF SCIENCE in Computer Engineering.

Department of Electrical and Computer Engineering

Thesis Advisor: *Dr. Chee-Wooi Ten #1*

Committee Member: *Dr. Zhaohui Wang #1*

Committee Member: *Dr. Gordon G. Parker #2*

Department Chair: *Dr. Daniel R. Fuhrmann*

Contents

List of Figures	ix
List of Tables	xiii
Acknowledgments	xv
Abstract	xix
1 INTRODUCTION TO ADVANCED METERING INFRASTRUCTURE	1
1.1 Hierarchical Structure of AMI network	3
1.2 AMR versus AMI	6
1.3 AMI Communication Infrastructure	8
1.3.1 “Smart” Meter	8
1.3.2 Setup of AMI Communication	9
1.3.3 Meter Data Management System (MDMS)	13
1.4 Survey on Current Deployment and Possible Improvements	14
1.5 Enhancement of Metering Infrastructure in Distribution Grid	17

2	CAMPUS DISTRIBUTION GRID	19
2.1	Current Status of AMI Deployment	20
2.2	Deployed Metering Infrastructure	23
2.3	Distribution Feeders	29
2.4	Substation Transformers	35
2.5	Backup Generating Units at MTU Substation	38
3	IMAGE EXTRACTION ALGORITHM FOR ELECTROMECHANICAL ANALOG METERS	45
3.1	Comparison between Three Different Metering Infrastructures	47
3.2	Campus Metering Testbed	52
3.2.1	Design of Timer Camera	53
3.2.2	Operational Mode of Mobile Devices	54
3.2.3	Pictorial Data from Electromechanical Meters	58
3.3	Data Extraction from Snapshot Images	60
3.3.1	Data Extraction for Electromechanical Analog Meters	60
3.3.1.1	Image Segmentation	60
3.3.1.2	Digital Image Preprocessing	62
3.3.1.3	Pointer Extraction Algorithm	65
3.3.2	Data Extraction for Energy Meters with Digital Unit Display	69
3.3.2.1	Digital Images Processing	69
3.3.2.2	Image Segmentation	70

3.3.2.3	Comparison Algorithm for Pixel Differences	70
4	CASE STUDY	73
4.1	Decision to Select an Unmetered Building	73
4.2	Test Case Setup	76
4.3	Study Results	78
5	CONCLUSION AND FUTURE WORK	83
	References	89
A	STATISTICAL RESULTS	99

List of Figures

1.1	Communication Infrastructure of AMI System.	4
1.2	Existing Analog Meter and the New IP-based Energy Meter. “See [1] for picture that this material is in the public domain.”	9
1.3	Communication Infrastructure of AMI System.	12
1.4	Flowchart of MDMS Working Process.	14
2.1	The Deployment Status of Campus AMI (Ten Buildings with IP-Based Building Meters). “The base map in this picture is captured from Google Map which is in the public domain.”	21
2.2	Deployment Status for Each Building with Annual kWh for Fiscal Year 2012-2013.	24
2.3	Computerized Management System for Deployed Metering Infrastructure.	25
2.4	Example of Web-Based User Interface for Substation Injection Points (UPPCO1 Meter).	26
2.5	Example of Web-Based User Interface for Phase-One Deployed Buildings.	27

2.6	Primary and Backup Feeders for Each Building.	30
2.7	Detailed Topology Connections of Three Feeders with Switch Open / Closed.	31
2.8	Frequency Disturbance Recorder (FDR) and GPS Antenna Place- ment. “See [2] for picture that this material is in the public domain.”.	33
2.9	Distances (in Feet) Between Buildings for All Feeders.	34
2.10	Location and Campus-Wide Backup Generators. “The base map in this picture is captured from Google Map which is in the public domain.”	38
2.11	Schematic for MTU Campus Substation.	39
2.12	Buildings with Local Backup Generators and Electrical Connections with Others.	40
2.13	The Current Topology of the Buildings with Local Generating Units and Frequency Disturbance Recorders (FDR) in Blue and Green Col- ors, Respectively. “The base map in this picture is captured from Google Map which is in the public domain.”	41
2.14	Clustering a Collection of Buildings with Local Generating Units based on Their Vicinity and Connectivity.	42
2.15	Potential Future Setup for a Networked Microgrid.	43
2.16	Cluster Numbering and its Total Capacity in kilo Voltage-Ampere (kVA).	44

3.1	Four Types of Energy Meters for Campus Distribution Grid: Type 1: Analog with Pointers. Type 2: Analog without Pointer. Types 3 and 4: Non-telemetered Digital Meters.	48
3.2	Flowchart of Timer Camera Design Algorithm.	54
3.3	Image Snapshots to the Cloud with Key Processing Elements. . . .	55
3.4	Metering Infrastructure for Campus Distribution Grid.	57
3.5	Proposed Simulation of Energy Consumption Using Sample Data. .	59
3.6	Image Segmentation in 4 Steps from (a) to (d).	61
3.7	Exported Images After Segmentation and Preprocessing.	64
3.8	Flowchart of Matrix Border Grayscale Detection Algorithm.	65
3.9	Intercepted Square Box with a Dial Plate Arrow within an Image. .	67
3.10	Digital Images Preprocessing and Image Segmentation in 5 Steps: (a) Original Image. (b) Grayscale Image. (c) Binarization Outcome. (d) Counter-color Outcome. (e) Analyzable Objects.	71
3.11	Flowchart of Pixel Differences Comparison Algorithm.	72
4.1	Four Types of the Remaining Unmetered Buildings.	74
4.2	Wi-Fi and Outlet Availability for Unmetered Buildings.	75
4.3	Actual Timer Camera Device in Operational Mode.	77
4.4	Energy Consumption of Building-20 208-V Circuit Between March 22, 2014 and March 30, 2014.	79

4.5	Energy Consumption of Building-20 480-V Circuit Between March 22, 2014 and March 29, 2014.	79
4.6	Average Consumption for Building-20 208-V Circuit.	80
4.7	Average Consumption for Building-20 480-V Circuit.	80
4.8	Consumption Percentage Piecharts for Buildings with AMI, Analog Meters, and Analog Meters with Proposed Method (Number 20).	82
A.1	(19) Chemical Sciences and Engineering Building.	101
A.2	(31) Douglass Houghton Hall (DHH).	102
A.3	(17) J. R. Van Pelt and Opie Library.	103
A.4	(38/39/40) McNair Hall.	104
A.5	(7) Electrical Energy Research Center (EERC).	105
A.6	(24) Student Development Complex (SDC).	106
A.7	(12) Minerals and Materials Engineering (M&M).	107
A.8	(8) Dow Environmental Science and Engineering Building.	108
A.9	(18) U. J. Noblet Forestry and Wood Products Building.	109
A.10	(37) Wadsworth Hall.	110

List of Tables

1.1	Comparison between AMI and AMR.	7
2.1	Phase-One Cyberinfrastructure Deployment with Distribution Trans- formers for Each Building.	37
3.1	Comparison of utility costs between electromechanical meters, IP- based “smart” meters, and the IE approach.	49
4.1	Error rate analysis	80

Acknowledgments

As I put this thesis together, I learned that there are more tasks than I originally expected that I have to do, compared with the class projects that I worked on in the past. This includes complying the guidelines of the graduate college requirements, providing ample time to the committee members to review my thesis prior the final oral examination, working on the practical problems that are so close that I can actually “see” them because most of the infrastructure is local. I realize that how challenging it can be to write a technical paper especially English is not my primary language – I learned to write succinctly and state my contribution to meet the requirements of graduate college as the partial requirement of the graduate degree.

I started my Master’s program since Fall 2012. I began working on this project in the summer of 2013 and compiling the work into this thesis sometime in the middle of summer. Over the past one year, I have been working closely with Mr. Gregory Kaurala to coordinate and manage the existing metering datasets from the IP-based “smart” energy meters from the ten buildings. I am grateful for his assistance and time to collect and coordinate the relevant metering information.

I value family and I always feel that it is important to have family comes first, then I will get stronger emotionally. Without the love and support from my parents, I would

not have come so far and I indeed am very appreciative of their encouragement.

While being a teaching assistant for most of my semester, I realize that time management is crucial particularly meeting project deadlines as well as coursework requirements. Research is always a subject that many have to innovate and we have to think outside of the box. While I find out that conducting literature survey, I gained the prospectives of what are the state-of-the-art out there at the same time I started to first learn how to reproduce their results and then to learn how to do it better. This is the learning process as a researcher in Master's degree on plan-A track that would sharp me better professionally. First off, I would like to express my deepest appreciation to my advisor, Dr. Chee-Wooi Ten, for providing professional development opportunities, support, feedback, and valuable advice to my research development. His mentorship and commitment in teaching and research exemplifies a role model for me. This work is a collaborative effort with him with constant interactions that concludes what we have accomplished thus far.

There are other faculty members at Tech would also set a good example for me to learn from. Dr. Chaoli Wang (who is now with the University of Notre Dame) advised me with technical aspects for improving the relevant algorithm and the accuracy of energy usage results. Dr. Gordon Parker provides his guideline for the editorial advice to suggest with some improvements on the journal article we were working on. This includes how to write well targeting on a very specific audience, particularly in

the technical description of formulas and figure captions to effectively communicate to the readers. All of my mentors have provided me great advices to improve the precision of my writing in this thesis.

Thanks to my colleagues who have been discussing with me on the challenging subject that provides me some directions on how to solve a problem. This includes generosity to provide their feedbacks with ideas throughout the development of this thesis. All of them deserve a mention here, especially, Mr. Wensheng Sun, Mr. Zilong Hu, Mr. Rashiduzzaman Bulbul, and Mr. Yonghe Guo, with all of them enrolled in the PhD program.

I also would like to express my appreciation to the writing coaches of Multiliteracies Center. They have been very helpful to proofread my thesis that corrected all my typographical and grammatical errors to the version that is “textbook” perfect.

Financially, I am very grateful to the Electrical and Computer Engineering Department and the Power and Energy Research Center (PERC) for the support of initial-phase metering deployment project.

And last, I would like to thank Drs. Zhaohui Wang and Gordon Parker as part of my defense committee to review my thesis. Upon completion of this degree, I intend to continue my doctorate here at Tech.

Abstract

In recent years, advanced metering infrastructure (AMI) has been the main research focus due to the traditional power grid has been restricted to meet development requirements. There has been an ongoing effort to increase the number of AMI devices that provide real-time data readings to improve system observability. Deployed AMI across distribution secondary networks provides load and consumption information for individual households which can improve grid management. Significant upgrade costs associated with retrofitting existing meters with network-capable sensing can be made more economical by using image processing methods to extract usage information from images of the existing meters. This thesis presents a new solution that uses online data exchange of power consumption information to a cloud server without modifying the existing electromechanical analog meters. In this framework, application of a systematic approach to extract energy data from images replaces the manual reading process. One case study illustrates the digital imaging approach is compared to the averages determined by visual readings over a one-month period.

Chapter 1

INTRODUCTION TO ADVANCED METERING INFRASTRUCTURE

In recent years, smart grid vision has been widely promoted to address the energy sustainability with integration of advanced sensors and technologies onto the existing power infrastructure. The current status of power grid has been improved with new regulations of energy policies with enhanced reliability. Through the rapid expansion of intelligent communication infrastructure, the vision varies from each country. For example, the authority of China has set ambitious goals to clearly achieve their top-down priorities to massively deploy phasor measurement units in substation network,

whereas in North America has the bottom-up approaches, i.e., to integrate renewable energy in transmission system as the same time deploy the “smart” IP-based meters in distribution networks. Overall, the vision has set a higher standards for electricity safety, energy usage efficiency, environmental protection as well as operational resiliency. Advanced metering infrastructure (AMI) is one of them has been prioritized for providing consumers with additional options for them to use energy at home. The interdisciplinary efforts with communication experts would revolutionize the power industry that has been referred as a “smarter” grid as a ultimate goal.

One benefit of being part of the AMI initiative is to enhance the communication between customers and utilities. This transition provides an option for consumers to decide when they would work on their laundry, when they will start charging their electrical car, when they should turn off the lights, etc. Recently, modern science and technology developed including the transition with the use of communication and information technologies, the promotion of environment protection procedures, and the upgrade of operating systems, the technological advance would tremendously improve AMI communication architecture. Other issues include asset management, energy conservation as well as emission reduction, largely deploying AMI systems would be part of the important milestones for the vision [3]. AMI is an integral of the modern communication infrastructure for distribution grid that will be connected with the dispatching control centers [4].

1.1 Hierarchical Structure of AMI network

AMI is a network management system consisted of “smart” IP-based meters installed in the side of users, the data management console located in the data monitoring center, and the communication network to transmit the relevant electricity information. The modern communication technology has been able to be extended to the home area network (HAN), local area network (LAN), and wide area network (WAN) to enhance the transmission efficiency in different regions with various area sizes.

Figure 1.1 demonstrates the fundamental structure of AMI. The “smart” meter has the ability to measure approximate real-time electricity information, e.g., the three-phase voltage and current, real and apparent power, frequency, and energy consumption. The collected data will transmit to the data management center via the pre-setting communication network. The data transmission network can be public networks or appropriate networks such as power line communications (PLC), fixed radio frequency (RF), and the power supply administration [5]. The relevant data collected from “smart” meters are received and stored in the data center which have to pre-set enough storage space, and then the gathered data will be sent to the management console for modeling and analysis. The data management system is capable of monitoring and supervising relative electricity information via Web browsers. In addition, the functions of AMI control and operation, dynamic electricity price billing,

and feedback of customer service can be achieved in this system. In order to improve the security level in the management port, there should always be a firewall between data reception and management system to ensure only users with special access have the ability to check and administrate relevant data. The bi-directional flow of information between the consumers and the customer billing center provides the data resolution up to 15 minutes per cycle [5].

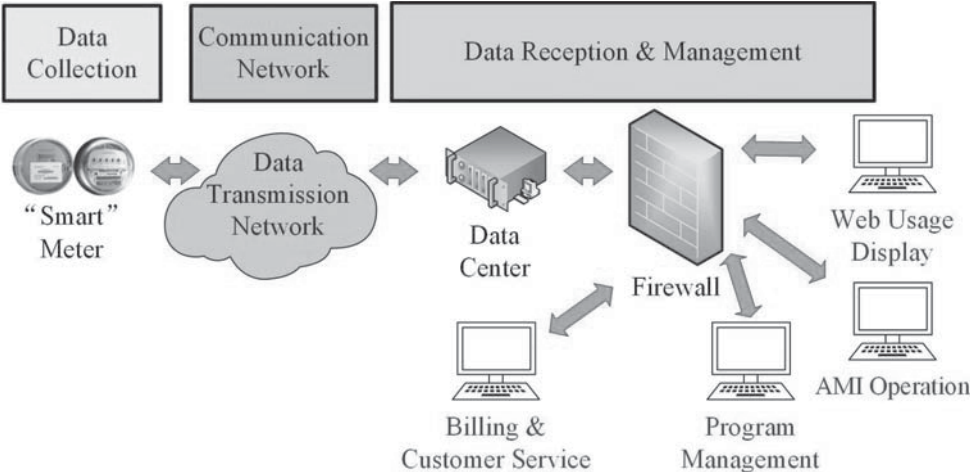


Figure 1.1: Communication Infrastructure of AMI System.

The AMI system is part of the communication framework for distribution grid. Initially, the automatic meter reading (AMR) is implemented to improve the metering accuracy as well as cost reduction of labor that would constantly for them to read the kWh information at consumers premier. As the relative communication technology advances and the interactivity between utilities and consumers increases, the advantages and benefits of AMI system has evolved from AMR to AMI with additional control variables on demand response. Below are the major benefits summarized for

AMI:

- 1) Utilization of AMI information between utilities and consumers for optimal energy usage.
- 2) AMI provides close-to-real-time information to utilities.
- 3) AMI also has demand response features that allows consumers to opt-in during the peak hours of the day/season.
- 4) AMI is a paradigm to share electricity usage information between consumers and dispatching control center when pricing scheme would affect their energy usage behavior [6].
- 5) The detection module for power quality can be setup in “smart” meter to facilitate inspection within a distribution system [7].
- 6) AMI would increase the system observability that can be used in operational mode and other application such as cross-domain data validation against cybertampering.
- 7) The increased system observability would help system dispatchers to pinpoint faulted segment of secondary distribution network [8].
- 8) Consumers would be able to make an economical decision based on the pricing information and their desire when/what to use energy.

1.2 AMR versus AMI

The major distinction between AMI and AMR is the control variables. While AMR would transmit energy usage information to the customer billing center, the AMI would enable the control capability between the utilities and customers if they choose to opt out from the peak load period that would be incentivized. The new paradigm would enable consumers to be more pro-active in participating the electricity market. Both AMR and AMI replace the site manual reading by utility crew. The features of AMR is similar as AMI, which it transfers the data of household energy consumption, meter status, as well as diagnostics to customer billing center mainly for collecting billing information [9, 10]. AMI is a predecessor of AMR that provides next-generation functionalities with IP-based metering solutions. Table 1.1 shows the differences between AMI and AMR. From the users and operational perspective, this table summarizes the important aspects of the system-large metering implementation for dynamic pricing market that would engage consumers participation. This IP-based metering solutions would also provide information to the consumers in order for them to make a sound, economical decision. As this is not internationally used for operational purpose, some approximation of instantenous values of the power consumption / energy usage would be sufficient enough for the collection of household billing information.

Table 1.1
Comparison between AMI and AMR.

	AMI	AMR
Data Collection	Collect data according to pre-set. Support real-time reading.	Typically gather data monthly, daily at most.
Communication Mode	Two-way Communication.	One-way Communication.
Benefited Parties	Engineering, operations asset-management, planning departments, customer service, billing, and metering [11].	Billing and metering.
User Operation	Users can manage the working time of devices and communicate with “smart” devices.	Not applicable.
Pricing Model	Dynamic prices.	Fixed prices.

Comparing between the two, the computational power has exponentially improved over last decade. The embedded system of the AMI devices can be designed with a more robust capability for communication. As the power of such device improves, including more information as well as with increased frequency of information exchange is desired. In addition to that, the functionalities of IP-based “smart” meters also include load control, prediction of potential fault location within the secondary network, event reports such as unavailability of the meters as well as firmware update for enhancing the functionalities of the IP-based meters. Most upgrades are being updated with patches for data security and reliability.

1.3 AMI Communication Infrastructure

The communication infrastructure of an AMI consists of the IP-based devices of “smart” meter, communication network between the customer billing center and the consumers as well as the servers of meter data management system (MDMS). These are the integral parts of an AMI system that are described in the next subsections.

1.3.1 “Smart” Meter

The IP-based “smart” energy meters are the instrumentation to transmit energy usage between customers and billing center. It provides the data transmission interface to connect communication network and the data acquisition unit. Figure 1.2 shows an example of electromechanical analog meter and IP-based energy meter depicted in Figures 1.2(A) and (B), respectively. Unlike the electromechanical analog meter, the “smart” meter displays digital numbers on its panel. Crew who visits the consumer premise site would understand how to interpret the angle of arrows on the display of the electromechanical analog meter.

The measurement variables of the IP-based meters include kilowatt hour (kWh), kilowatt (KW), voltage (V), or ampere (A). Pre-setting the measuring interval for 10

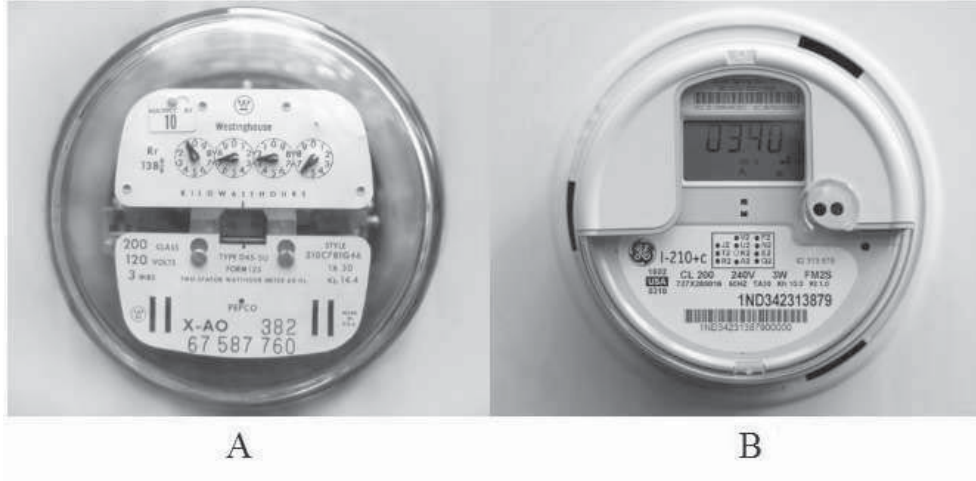


Figure 1.2: Existing Analog Meter and the New IP-based Energy Meter.
“See [1] for picture that this material is in the public domain.”

or 15 minutes, and then utilizing the open two-way communication for the purpose of monitoring, information verification, and diagnostics. These meters may have the privileges to receive real-time dynamic electricity price from the market authority that would include demand response features.

1.3.2 Setup of AMI Communication

As the only medium during information transfer, the AMI communication network provides secure and effective services to ensure data exchange. Two communication modes, wired or wireless, are available in AMI communication system. Regarding the wired mode, three main methods, which are serial communication, ethernet, as well as optical fiber communication, are described briefly below.

- 1) *Serial Communication*: This communication mode is originally designed to transfer data over large distances. In the AMI system, the IP-based meter sends data one bit at a time, sequentially, over one data cable connected with the serial communication port in the meter. Sometimes, the serial communication can also be utilized with other modes, e.g., ethernet or the optical fiber [12].

- 2) *Ethernet Communication*: As one of the most economical and widely used modes in networking technologies for local area (LAN) or larger networks, ethernet can be used in the IP-based meters. The data cable connects the ethernet interface in the meter with the data collector for wired communication. Optimizing data transfer across multiple sites, some network protocols are available at the ethernet level include transmission control protocol (TCP) or ModBus [13]. ModBus can accelerate data transfer by integrating relevant electricity information into the data module installed in the IP-based meters [14].

- 3) *Optical Fiber Communication*: This mode is the optimized technology from ethernet. This method performs rectilinear data transfer via converting electronic signals to light signals, which could send data packages to destinations with different distances immediately [15]. The major disadvantage of this method is the exorbitant price. Generally, an AMI system collects data from a region first and then transmit via optical fiber.

As a practical matter, an AMI system needs wireless communication mode to provide continuous, fast, and stable data transfer for optimizing datacenter operations within local areas as well as wide areas. Two wireless methods extensive used in the AMI system are Wi-Fi and embedded system. Below will describe these two methods roughly.

1) *Wi-Fi*: It is the most common technology in wireless communication. The implementation procedure in AMI is to establish wireless base stations that have to guarantee the provided network is capable of covering all IP-based meters. The base stations connected with each other through the network bridge between different wireless access points [16]. In addition, the choice of meter installation site is important. Before install the wireless devices, a site survey of each installation location has to detect the strength of signal and interference around each meter to make sure the communication quality.

2) *Embedded System*: Comparing with other wireless communication modes, embedded system is a comprehensive method. Besides more stable information transmission, it allows users to combine multiple communication modes based on their definite requirements to complete the data transfer [17]. The embedded system can provide the optimal solution for wireless communication in an AMI system.

In addition, the global system for mobile (GSM), general packet radio service (GPRS), and 3G/4G network could also be applied in AMI system [18]. Since the exploitation of AMI system, the option of advanced communication technologies has become increasingly complex. The implementers should consider more circumstances such as reliability, operating maintenance, or capital spending to select the suitable communication mode. The communication of AMI rely on three networks: home area network (HAN), neighborhood area network (NAN), and wide area network (WAN) [19]. The basic communication infrastructure of an AMI system is illustrated in Figure 1.3.

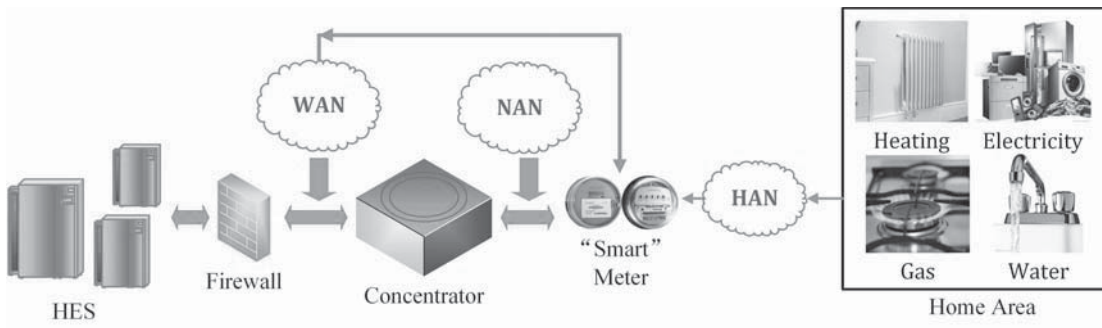


Figure 1.3: Communication Infrastructure of AMI System.

Regarding a complete AMI system, the measured information which could be transmitted is not just electric power data; it could also gather the consumption information of water, gas, or heating. The main function of HAN is to integrate additional data and send them to relevant “smart” meters. Then, the data is sent through NAN which is sometimes also identified as local area network (LAN) or field area network (FAN) [19] to connect meters and concentrators. In the end, the WAN will connect the concentrator or the single “smart” meter to the head end system (HES) which has the ability to communicate with meters directly and also could be known as a

meter control system [19]. Between WAN and HES, there will always be a firewall or special approval protocol to guarantee the security of data transmission.

1.3.3 Meter Data Management System (MDMS)

As the key component in the AMI system, the meter data management system (MDMS) performs long term data storage and monitoring for the vast quantities of usage information delivered by IP-based meters. The data is typically imported to the MDMS first for preprocessing, e.g., verification, filtering, and disposing, before making it available for billing and analysis. Also, the MDMS can interact with some functional systems such as a power on or off control system or a dynamic prices system [20]. The working procedure of the MDMS is shown in Figure 1.4. The MDMS can obtain the timely data report to do the energy consumption forecasting, load capacities reporting, and customer service feedback [21].

Making full use of the gathered information is an important benefit of the AMI system. Apart from compiling the timely data, the MDMS can also maintain the data integrity even without data transfer, which means the MDMS can store the measured data under network disconnecting situation. Currently, many electrical companies are planning to establish the MDMS based on the existing metering system to promote work efficiency and performance.

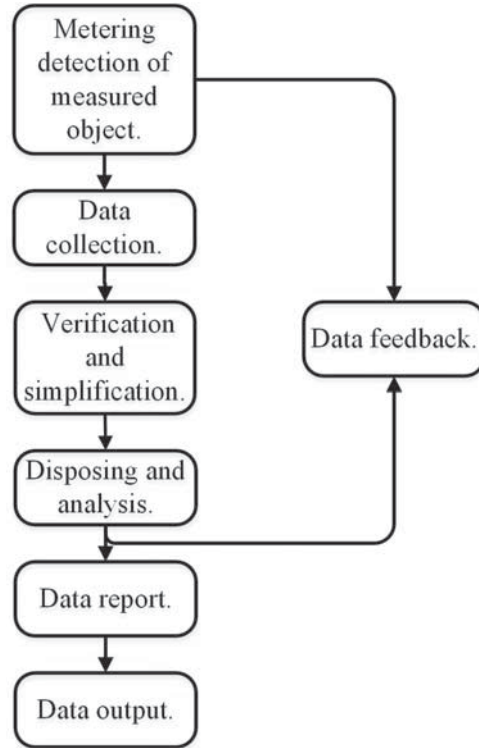


Figure 1.4: Flowchart of MDMS Working Process.

1.4 Survey on Current Deployment and Possible Improvements

With the improvement of automation and practical ability in management of the electric power business, partial function of the AMR system has trended toward AMI system features that evolved from simple meter reading performance to be capable of monitoring the real-time information, assessing the electricity, remote controlling, automatic billing and other features. For the proven and stable electricity business, the AMR occupies a large proportion of market shares while the AMI technology that

only has the operational experience of three to four years which means it is still in the probational stage. The future deployment of an AMI combines with the problems which occurred in campus AMI system.

- 1) Before confirming the service model and preliminary scheme, we need to complete the user requirement analysis and feasibility survey to reach the goal of resources and capital conservation to improve work efficiency. For example, at Michigan Tech, the first-phase deployment of the AMI system has been accomplished, and it has been capable of providing high percentage coverage of system observability. When the second-phase deployment is implemented successfully, the AMI system will be able to monitor more than 80 percent of the energy consumption information. That will leave around 17 buildings dispersed located on campus that deploy the rest of the electricity data. The constructor will not deploy the AMI structure in these buildings based on the principles of maximum efficiency and implementation difficulty.

- 2) Communication network is the core part of the whole AMI system because it is the only medium to connect meters, monitoring terminals, the database, and the data management system. How to improve the performance in a communication network that contains security and stability should be one of the major steps for future development of the AMI system. During the summer in 2013, the communication network of the AMI system in Michigan Tech was made public because

of the upgrade of the campus network. Anyone who can log into the Michigan Tech account can also observe the data management system and supervise the operating status of the power supply system without any restrictions. Under normal circumstances, only the administrative users and managers have the access via passing a virtual private network (VPN) identification.

- 3) An integral system combined with hardware and software, also it should have an alarm system to ensure valid and efficient operating. An advanced feature of an AMI system is the telemetered capability to feedback with fault indicators that trigger a disturbance alarm to the data center in real-time. The current AMI system can only estimate the running states by checking metering information. From the last half of 2013 to present, an error appeared in the UPPCO meters; the connection of the network interface adapter in the meter was disconnected. The power information can be detected in an input terminal rather than an output port, which means the data can be shown to the power supply company but can not display in the campus internal database. We lost the real-time monitoring function of the overall consumption.

1.5 Enhancement of Metering Infrastructure in Distribution Grid

In the metering infrastructure, “smart” meters in the power grid could be treated as sensors or measuring points spread over the whole network. Using communication facilities and information system provided by the electric company or relevant department, AMI is capable of offering the much more timely and effective measurement. Furthermore, the communication network in the AMI system can support some advanced applications in a power grid, e.g., power distribution automation and automated management in a substation. In the meantime, the operating state could be estimated and checked by the presented data from AMI. Therefore, the AMI system is regarded as the first step to establish smart power grid. After the implementation of AMI, the electricity providers will progressively achieve advanced capabilities such as distribution operation, asset management, and a series of analysis and modeling.

Chapter 2

CAMPUS DISTRIBUTION GRID

As the first major milestone and the fundamental structure of the overall smart power grid, AMI measures, collects, and analyzes data about energy usage and power quality from the terminal “smart” meters, and achieves valid data exchange between the distribution dispatching center and customer billing network [22, 23]. In most US power utilities, the coverage of the AMI system has risen from 8.7 percent in 2010 to about 30.2 percent in 2013 [24] and the reliability rate is around 99.7 percent [25]. Due to the critical role of information exchange in distribution grids, real-time data acquisition is one of the primary tasks in a distribution grid that constantly pulls the usage information to a central database using IP-based communication network [26].

2.1 Current Status of AMI Deployment

The current status of AMI deployment in Michigan Tech is still in a fledging period. The initial AMI deployment was commissioned on 10 campus buildings since the first quarter of 2012. These metered buildings sometimes represent more than half of energy consuming loads and, after the deployment of the second-phase, the AMI system will cover more than 80 percent of campus power consumption information. Due to the budgetary constraints, deploying “smart” electronic meters for the remaining percentage of unmetered buildings may not be cost efficient. Although the accomplished infrastructure provides high percentage coverage of system observability, the energy usages for those buildings fluctuate over time. The current structure of completed AMI has the ability to provide the observation of up to 65% of the energy usages for the campus distribution system.

Figure 2.1 illustrates the campus distribution grid. In this figure, the dark grey circles represent accomplished phase-one buildings with “smart” IP-based meters. The capital A module shows the substation in this grid while B represents the terminal port of the system. There is one substation and four generating units in building 41 which is also the facilities management site. There are three existing distribution feeders and each building is connected to a primary feeder and a backup feeder. As shown in the map, there are many remaining buildings needed to be considered in

the future to achieve entire grid intellectualization at campus-wide. The numbers on this map represent building numbers.

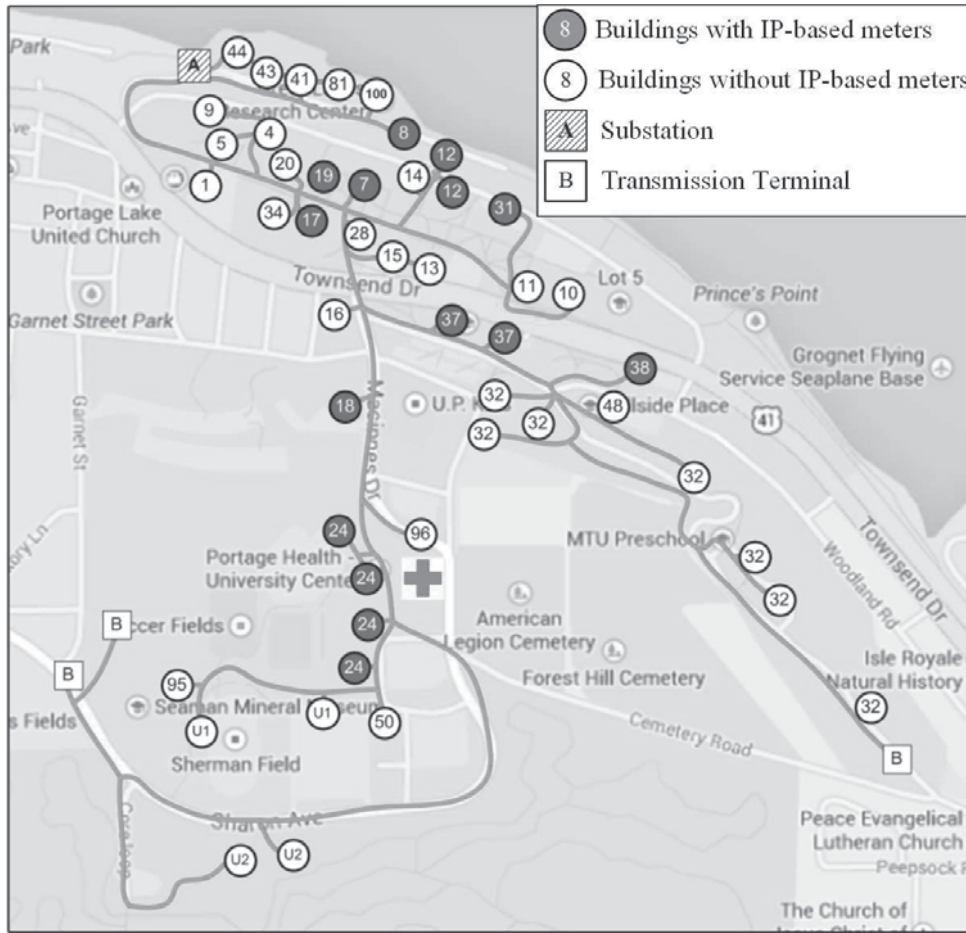


Figure 2.1: The Deployment Status of Campus AMI (Ten Buildings with IP-Based Building Meters). “The base map in this picture is captured from Google Map which is in the public domain.”

Figure 2.2 shows the deployment status of campus distribution grid for the fiscal year of 2012 to 2013, which also contains the building numbers and corresponding names, annual and average energy consumption, and the energy consumption percentage of each building.

According to this figure, the accomplished phase-one AMI system covered around 63 percent of power consumption in the whole campus power grid for last year, while the observation of both phase-one and phase-two deployments will rise to around 83 percent. That would be the initial target of the campus AMI construction and we may not continue to install AMI in the remaining buildings anymore because of the consideration of efficiency and cost reduction. There will be more than 15 buildings left which only hold less than 20 percent of campus consumption observation. Although the energy usage of Daniell Hights (DH) is about 5 percent, which is large enough to regard, this building represents the campus living quarters which consists of many dispersive units. Consulting campus-wide distribution grid map, we could discover the region of DH is large and the locations of units are scattered. The AMI construct process in DH would be inconvenient and have a high cost.

Over the past decade, the annual energy expenditure for campus energy usage is estimated to be millions of dollars consistently for all campus buildings. Determining how to promote energy consumption awareness has been one of the major steps for reducing energy usage. With the accurate and timely information, the monitoring element has the capacity to detect energy quality and running states of the distribution system while the management console will be able to realize troubleshooting and electricity controlling [6, 27, 28]. This means that the distribution substation can guarantee high-efficiency electricity supply and control the power distribution capacity according to the real-time data feedback to reach the goal of energy conservation

[29].

2.2 Deployed Metering Infrastructure

The real-time data acquisition ability is one of the prime advantages in a distribution grid. The IP-based meter is one of the basic facilities for collecting, processing, and communicating real-time data in modern smart power grids [30]. The implemented intelligent structure with IP-based meters in the campus distribution grid is monitored by the AX supervisor which is a flexible network server applied in operations where multiple Niagara AX controllers based on Java application control engine (JACE), can be networked together [31]. Figure 2.3 is the architecture of data acquisition system for metering campus distribution loads using AX supervisor. The timely energy consumption information will be displayed on the energy meter as well as uploaded to the Internet through the IP-based Internet link module (ILM) [32]. Within the existing system, the IP-based metering data could be browsed and supervised using a web supervisor and browser through specific virtual private network access and then saved to the campus data server.

	Num	Name	Annual Energy kWh	Average Annual kWh	Total %	
Phase 1	Existing	37	Wadsworth Hall	2,948,727	336.61	9.28%
		38/40	McNair Hall	781,205	89.18	2.46%
		31	Douglas Houghton Hall	436,236	49.8	1.37%
	Phase 1(a)	8	Dow Env. Sci. and Engg. Building	3,756,535	428.83	11.82%
		12	Minerals and Materials (M&M) Engineering	2,415,005	275.69	7.60%
		19	Chemical Sciences and Engineering Building	1,758,005	200.69	5.53%
		18	U. J. Noblet Forestry & Wood Products	1,523,728	173.94	4.79%
		17	J. R. Van Pelt and Opie Library	1,488,891	169.96	4.68%
	Phase 1(b)	24	Student Development Complex (SDC)	1,903,834	217.33	5.99%
		7	Electrical Energy Resources Center	1,797,805	205.23	5.66%
		24	Ice Arena (SDC)	1,229,887	140.4	3.87%
	Total Metering Coverage for Phase 1:			20,039,858	2287.66	63.06%
Future Deployment	10	Mechanical Engg. & Engineering Mechanics	1,537,124	175.47	4.84%	
	15	Fisher Hall	751,665	85.81	2.37%	
	34	Memorial Union Building	1,000,512	114.21	3.15%	
	1	Administration	504,165	57.55	1.59%	
	14	Grover C. Dillman Hall	445,884	50.9	1.40%	
	11	Walker Arts and Humanities Center	789,125	90.08	2.48%	
	12	Benedict Lab	346,176	39.52	1.09%	
	28	Rekhi Hall	771,563	88.08	2.43%	
	10	Rozsa Center for the Performing Arts	207,205	23.65	0.65%	
Total Metering Coverage for Future Deployment:			4,816,295	549.81	83.05%	
Remaining	32	Daniell Heights	1,640,007	187.22	5.16%	
	96	Portage Health Center	221,000	25.23	0.70%	
	41	Central Heating Plant	185,521	21.18	0.58%	
	5	Academic Offices	120,973	13.81	0.38%	
	9	Alumni House	108,216	12.35	0.34%	
	44	Facilities Motor Pool	103,365	11.8	0.33%	
	50	Gates Tennis Center	108,265	12.36	0.34%	
	4	ROTC Building	60,487	6.9	0.19%	
	24	Fitness Center	61,087	6.97	0.19%	
	16	Public Safety	5,741	0.66	0.02%	
	13	Hamar House	30,384	3.47	0.10%	
	43	Lakeside Laboratory	11,209	1.28	0.04%	
	81	Gen Building	134,370	15.34	0.42%	
	48	Hillside Hall	696,181	79.47	2.19%	
	100	Great Lake Research Center	1,840,756	210.13	5.79%	
	U#1	SDC Lights	21,140	2.41	0.07%	
	U#2	Sharon Ave.	38,260	4.37	0.12%	
Total Annual kWh:			31,780,239	3,628	100.00%	

Figure 2.2: Deployment Status for Each Building with Annual kWh for Fiscal Year 2012-2013.

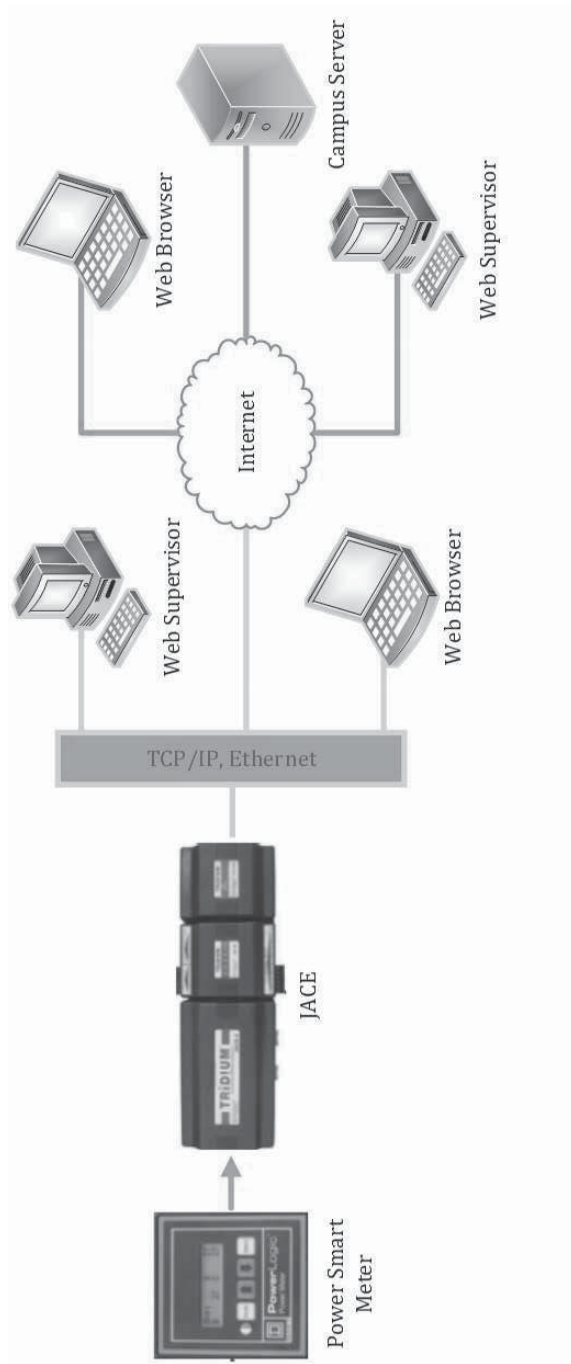


Figure 2.3: Computerized Management System for Deployed Metering Infrastructure.

The monitoring interface of the web supervisor is capable for observing measurements with different units. All of the observation is useful for observing the real-time consumption and estimating the operating status. Figures 2.4 and 2.5 illustrate the web user interfaces of measurement variables for the phase-one deployed buildings and UPPCO meter, which is applied for monitoring campus total energy consumption.

UPPCO1 Meter












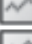









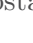
Total_KWH	984999783308E32	
Total_KVarH	0.0 kVA-hr	
LastCalcKW	0.0 kW	
LastCalcKVar	0.0 kvar	
InstKW	0.0 kW	
InstKVar	0.0 kVA-hr	
InstKVA	0.0 kVA	
Frequency	0.0 Hz	
AmpsPhaseA	0.0 A	
VoltsPhaseA	0.0 V	
AmpsPhaseB	0.0 A	
VoltsPhaseB	0.0 V	
AmpsPhaseC	0.0 A	
VoltsPhaseC	0.0 V	
THD_A_Amps	0.0	
THD_A_Volts	0.0	
RealtimeInstKW	3221279488.0 kW	
ProjectedInstKW	0.0 kW	
AccumulatedInstKW	0.0 kW	
RealtimeInstKVA	-0.0 kVA	
ProjectedInstKVA	-0.0 kVA	
AccumulatedInstKVA	0167556649827E37	

Figure 2.4: Example of Web-Based User Interface for Substation Injection Points (UPPCO1 Meter).

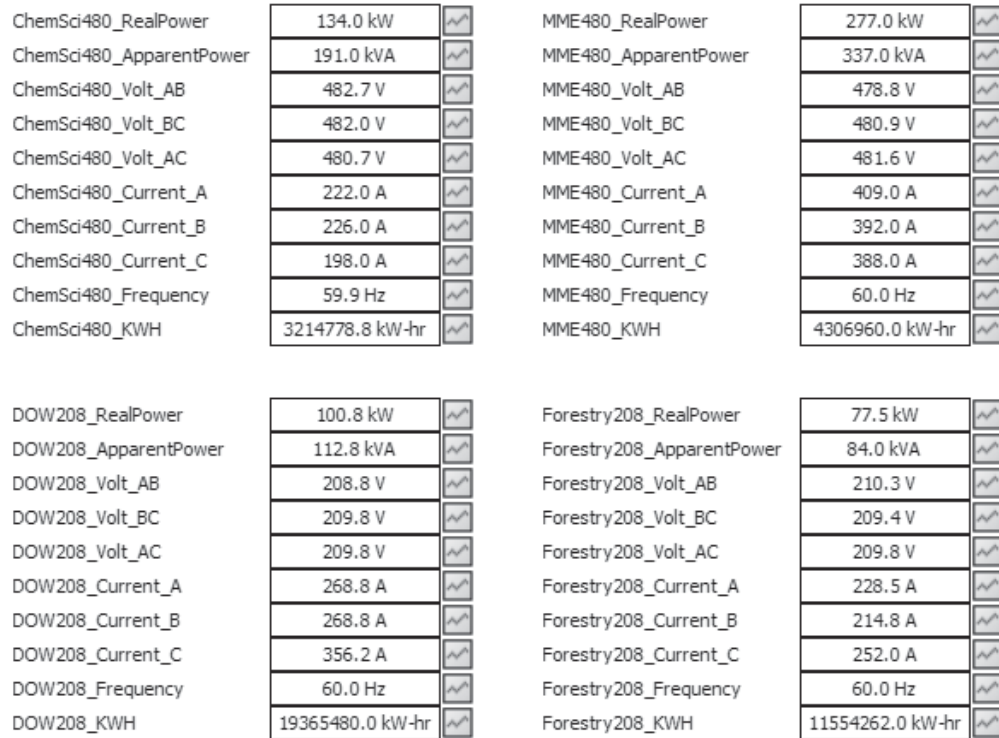


Figure 2.5: Example of Web-Based User Interface for Phase-One Deployed Buildings.

These two figures depicted the web supervisor to observe the usage information including real power, apparent power, three phases voltages and currents, frequency, and energy for each metered building. Also, we can check and download needed data based on different time durations which contain last year, year to date, last month, last week, yesterday, and the current day. The time interval of each measured data is 10 minutes. Furthermore, there are two UPPCO meters in the campus power supply substation but only one on working state at one time. In addition, five buildings which include the Chemical Engineering building, Minerals and Materials (M&M) Engineering building, Dow Environment Science and Engineering building, Electrical Energy Resources Center (EERC), and U. J. Noblet Forestry and Wood

Products building are constructed with two types of transformers which are applied with 208-V and 480-V separately. The transformer 208-V is primarily responsible for consumption limited electrical appliances such as light and power outlets, while the transformer 480-V is in charge of large electric facilities like air conditioning and laboratory equipment.

For security reasons to restrict the critical information of the campus metering database, the administrative users can manage the systems by tunneling through virtual private network (VPN) connection to campus intranet [33, 34]. Within the campus Intranet, subnets of different buildings are connected and are routed through the campus-wide communication backbone network to other internal networks for real-time information sharing. As mentioned, due to the budgetary constraints, deploying IP-based meters for the remainders of unmetered buildings may not be cost efficiency. Inventing a new method with reasonable price which is to increase a greater number of metering points for the lower priority buildings that pictorially acquire energy information from existing electromechanical meters. Instead, dedicated IP-based energy meters is necessary and the proposed framework will be described in detail in Chapter 3.

2.3 Distribution Feeders

The campus substation is the node that connects the power injection sources from UPPCO transmission network to three distribution feeders. Figure 2.6 demonstrates current feeder operating status for each building in the campus distribution grid. Every building in this system is electrically connected either by one of the two feeders at a time, which one connected as primary and the other as backup.

The detailed topology connections of three feeders in campus distribution grid is shown in Figure 2.7, where red line represents feeder one, green represents feeder two, and blue as feeder three. The connections in between each building and feeders are connected with switches.

NUM	Name	Feeder 1	Feeder 2	Feeder 3
2	Substation	ON	ON	ON
37	Wadsworth Hall	OFF	ON	
38/39/40	McNair Hall	ON	OFF	
31	Douglas Houghton Hall	OFF	ON	
8	Dow Env.	OFF	ON	
7	Electrical Energy Resources Center	ON	OFF	
10	Rozsa Center	ON	OFF	
32	Daniel Heights	ON	OFF	
100	Great Lakes Lab	ON	OFF	
48	Hillside Hall	ON	OFF	
41	Central Heating Plant	ON	OFF	
43	Ground Maintenance	ON	OFF	
81	Power Generation Building	ON	OFF	
11	Walker Arts and Humanities Center	ON	OFF	
12	M&M Eng.	ON		OFF
18	Forestry	ON		OFF
20	Mechanical Eng. & Eng. Mechanics	ON		OFF
15	Fisher Hall	ON		OFF
14	Grover C.Dillman Hall	ON		OFF
28	Rekhi Hall	ON		OFF
6	ANNEX Building	OFF		ON
13	Hamar House	ON		OFF
5	Academic Offices	OFF		ON
4	ROTC Building	OFF		ON
9	Alumni House	OFF		ON
12	Benedict Lab	ON		OFF
16	Public Safty	ON		OFF
19	Chemical Sci.&Eng.		OFF	ON
17	Library		OFF	ON
24	SDC		ON	OFF
24	Ice Area		ON	OFF
34	Memorial Union Building		OFF	ON
1	Administration		OFF	ON
50	Gates Tennis Center		ON	OFF
96	Portage Health Center		OFF	ON
U#1	SDC Parking Lot		ON	OFF
U#1	Fitness Center		ON	OFF
U#1	SDC Lights		ON	OFF
U#2	Sharon Ave.		ON	OFF

Figure 2.6: Primary and Backup Feeders for Each Building.

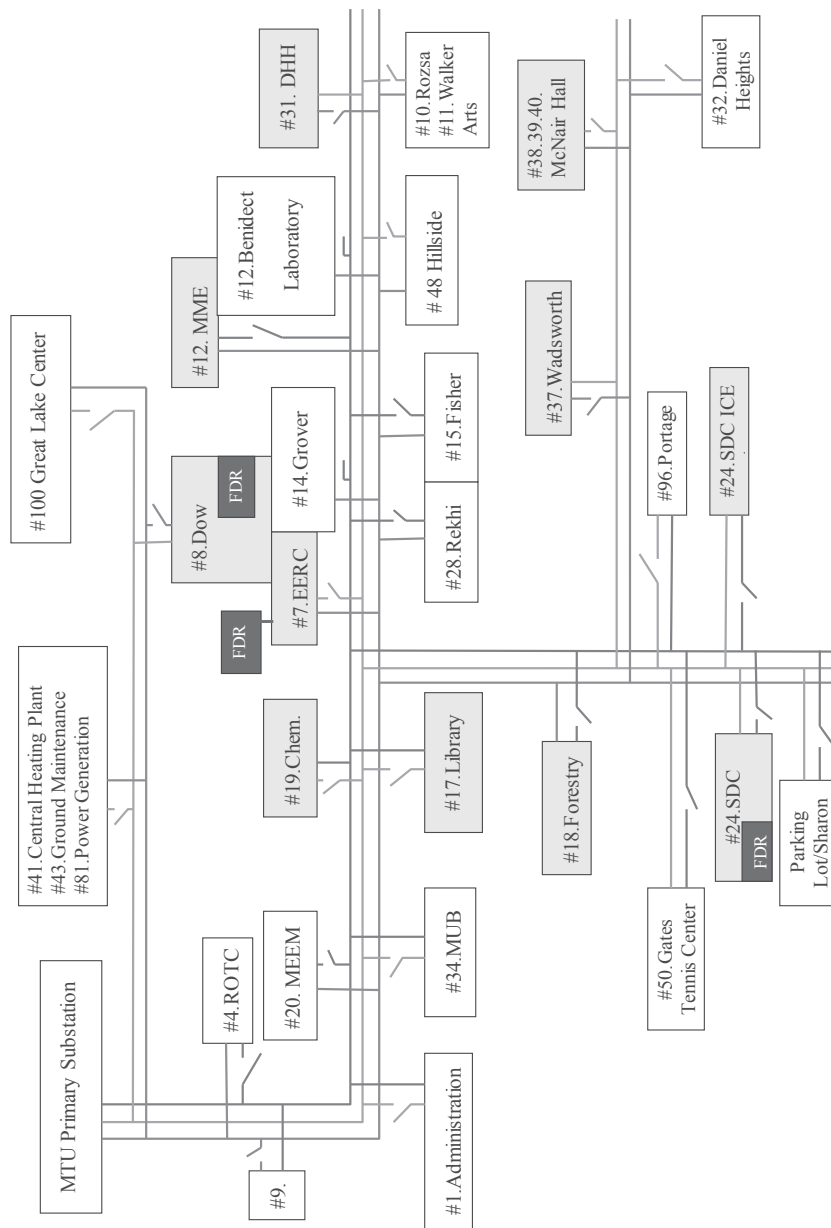


Figure 2.7: Detailed Topology Connections of Three Feeders with Switch
Open / Closed.

In this diagram, yellow blocks express the phase-one buildings with IP-based meters. There are three purple rectangles contained by buildings 7, 8, and 24 which represent frequency disturbance recorder (FDR). The FDR is connected for transmitting frequency information remotely via the Ethernet on 110V or 220V charge outlet [2]. The EERC has also served as a host site for the Upper Peninsula of Michigan. Its communication backbone is under frequency monitoring network (FNET) by the University of Tennessee Knoxville from EERC building. The other two FDRs are installed in the first floor of Dow Environment Science and Engineering building and the power control room in Student Development Complex (SDC). Taking EERC building as an example, one of the three FDRs is located on 6th floor of EERC. The EERC is connected to feeder 2 that serves the building consumption. Figure 2.8 illustrates the material object of a FDR device and antenna setting. The relevant switches and buttons are back of the device. The front lights only indicate the working state and the measured values are shown in the grey screen. The signal receiver and emitter in antenna shown in this figure should be placed around the area with better GPS reception.

During power distribution and transmission, the power loss in feeders should also be considered for loads modeling and estimating. In order to obtain the information of power loss, it is necessary to measure the actual distance of feeders between each building and the substation. Making the substation as the base and dividing all campus buildings by three different feeders, we labeled the concrete feeder distance

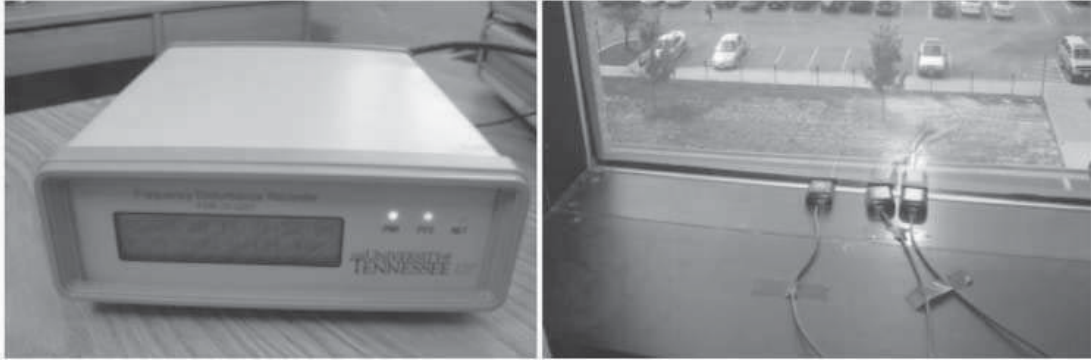


Figure 2.8: Frequency Disturbance Recorder (FDR) and GPS Antenna Placement. “See [2] for picture that this material is in the public domain.”.

between each conjunction node by field measurement in Figure 2.9 where the unit of distance is foot, the dark circles represent phase-one deployed buildings, and the capital “F” represents FDR in this distribution system.

In Figure 2.9, we could find the feeders with the longest length is from the substation to building 95 and the value is only 6147 foot which is less than 1.2 mile. The feeder utilized in campus-wide grid is named “AETNA INS WIRE 2AWG CU EPR 15KV 133 Percent INSUL LEVEL (220MIL)” that the resistance parameter is 0.964 /mile [35]. Doing a simple calculation, even the resistance in the longest part of the feeder is small enough, which means the power loss in this grid is too insignificant to consider.

2.4 Substation Transformers

As shown in the distribution grid map, phase-one cyberinfrastructure deployment includes the selected 11 buildings. The installation and implementation of these new devices is based on the load survey for each building per month by the facilities crews. The primary focus of this phase is to monitor the ongoing campus-wide energy usage by system operators in the control room. The selection of these locations includes coordination with campus electricians in order to determine the type of metering devices required. Depending on the manufacturer specifications of the instruments, the connection type follows the instrumentation at the secondary side of distribution transformers with a network interface provided via a Modbus connection. However, the flexible current transformer (CT) connection type requires an additional three sets of instrumentation for the two distribution transformers in each building with

six total for both secondary sides of transformers, i.e., 480-V and 208-V. Table 2.1 below shows detailed information of transformers in phase-one cyberinfrastructure deployment.

Table 2.1
Phase-One Cyberinfrastructure Deployment with Distribution
Transformers for Each Building.

Building	kVA	Voltage(V)	High Voltage	Low Voltage	Impedance(%)
MME 208	750/1000	12470Δ-208Y/120	95	10	5.95
MME 480	1500/2000	12470Δ-480Y/227	95	10	5.62
DOW 208	750/1000/1333	12470Δ-208Y/120	95	10	6.15
DOW 480	1500/2000	12470Δ-480Y/227	95	10	5.74
EERC 208	1000/1333	12470Δ-208Y/120	95	10	5.99
EERC 480	1500/2000	12470Δ-480Y/227	95	10	5.86
SDC 480	750	12470Δ-480Y/227	95	10	5.4
Ice Area 480	1000/1333	12470Δ-480Y/227	95	10	5.62
Forestry 208	500/667/888	12470Δ-208Y/120	95	10	5.89
Forestry 480	750/1000/1333	12470Δ-480Y/227	95	10	5.7
Library	1000	12470Δ-480Y/227	95	10	5.61
ChemSci 208	500	12470Δ-208Y/120	95	10	5.21
ChemSci 480	1000	12470Δ-480Y/227	95	10	5.5

2.5 Backup Generating Units at MTU Substation

In case of a fault or an emergency occurs at injection sources that could not meet the power usage requirements of facilities management. There are four backup generators connected in parallel to the campus substation to improve the reliability. Figure 2.10 illustrates the location of these local backup generators. Considering the appropriate distance between the backup generators and the substation, the four backup generators are set at the Central Heating Plant Building, which would be convenient for protecting and monitoring. The number of this building is 41 and the location of it has been indicated with a red arrow on the partial campus map. Figure 2.11 shows the schematic of the campus substation. The two UPPCO buses can transform their operating status via the tie switch in between them.

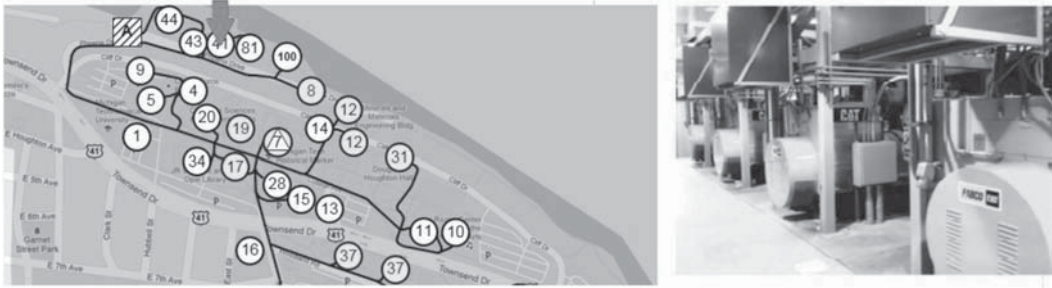


Figure 2.10: Location and Campus-Wide Backup Generators. *“The base map in this picture is captured from Google Map which is in the public domain.”*

The backup generators for each building are summarized in Figure 2.12 in kilo Volt-Ampere (kVA). Notice that not every building has backup generator. Those rows with

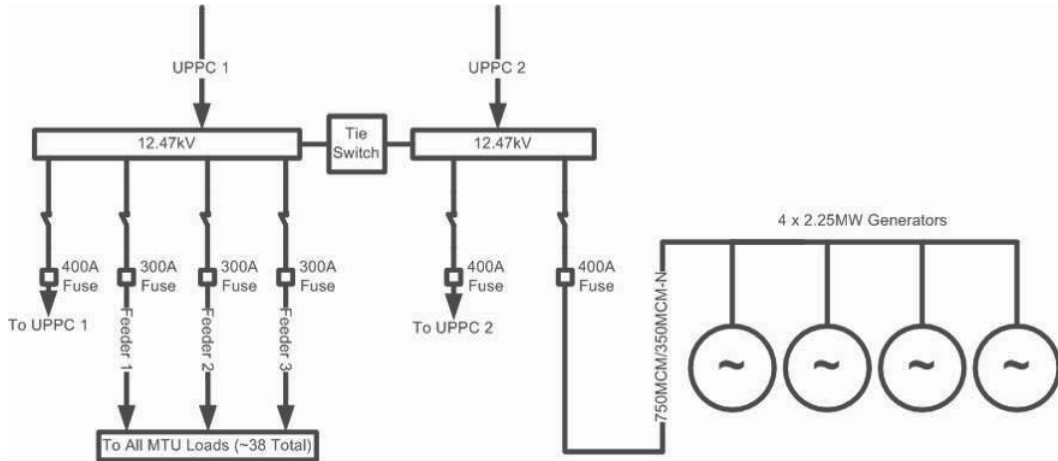


Figure 2.11: Schematic for MTU Campus Substation.

same color share with one backup generating unit; four different colors represents the four backup generators. Some buildings have their independent power source for backup that does not share with other buildings, e.g., buildings 38, 40, 12, 24, and 34. These buildings usually are equipped with a smaller unit.

The blue circles in Figure 2.13 represent the buildings have generators. Those building generators are only for emergency life safety purpose. During the power outage, they will be adequately used to light up the corridors, to start pumps, or sometimes for one elevator to operate. All of the metered buildings have generators. The backup generation rating ranges are from 125 kVA to 569 kVA and the total rating for these generators are around 2.3 Mega Volt-Ampere (MVA), while the average load of system is around 4.5 MVA.

The generators could not only provide the emergency power for the corresponding buildings, they also supply the power to their adjacent buildings sometimes. Figure

		No.	Name	Backup Generation (kVA)	
				Local	Access to
Phase I	Existing	37	Wadsworth Hall	188	0
		38/40	McNair Hall	156	0
		31	Douglas Houghton Hall	100	0
	Phase I(a)	8	Dow Env. Sci. and Engg. Building	0	565
		12	Minerals and Materials (M&M) Engineering	125	0
		19	Chemical Sciences and Engineering Building	188	0
		18	U. J. Noblet Forestry & Wood Products	188	0
		17	J. R. Van Pelt and Opie Library	569	0
	Phase I(b)	24	Student Development Complex (SDC)	144	0
		7	Electrical Energy Resources Center	188	0
		24	Ice Arena (SDC)	94	0
	Future Deployment	20	Mechanical Engg. & Engineering Mechanics	188	0
15		Fisher Hall	0	569	
34		Memorial Union Building	71	0	
1		Administration	0	188	
14		Grover C. Dillman Hall	-	-	
11		Walker Arts and Humanities Center	125	0	
12		Benedict Lab	-	-	
28		Rekhi Hall	0	569	
10		Rozsa Center for the Performing Arts	0	125	
95		Advanced Technology Center	-	-	
Remaining	32	Daniell Heights	-	-	
	96	Portage Health Center	-	-	
	41	Central Heating Plant	565	0	
	5	Academic Offices	-	-	
	9	Alumni House	-	-	
	44	Facilities Motor Pool	0	565	
	50	Gates Tennis Center	-	-	
	4	ROTC Building	-	-	
	24	Fitness Center	-	-	
	16	Public Safety	-	-	
	13	Hamar House	-	-	
	43	Lakeside Laboratory	-	-	
	81	Gen Building	-	-	
	48	Hillside Hall	-	-	
100	Great Lake Research Center	-	-		

Figure 2.12: Buildings with Local Backup Generators and Electrical Connections with Others.



Figure 2.13: The Current Topology of the Buildings with Local Generating Units and Frequency Disturbance Recorders (FDR) in Blue and Green Colors, Respectively. “The base map in this picture is captured from Google Map which is in the public domain.”

2.14 illustrates the current clusters with generating units on campus buildings. Each cluster shared one generator. The primary requirement for each generator is to ensure the adequate power supply. Except that, the deployment of power supplies varies depending on the topology of the grid network.

Figure 2.15 demonstrates the new microgrid clusters and future studies. A generator

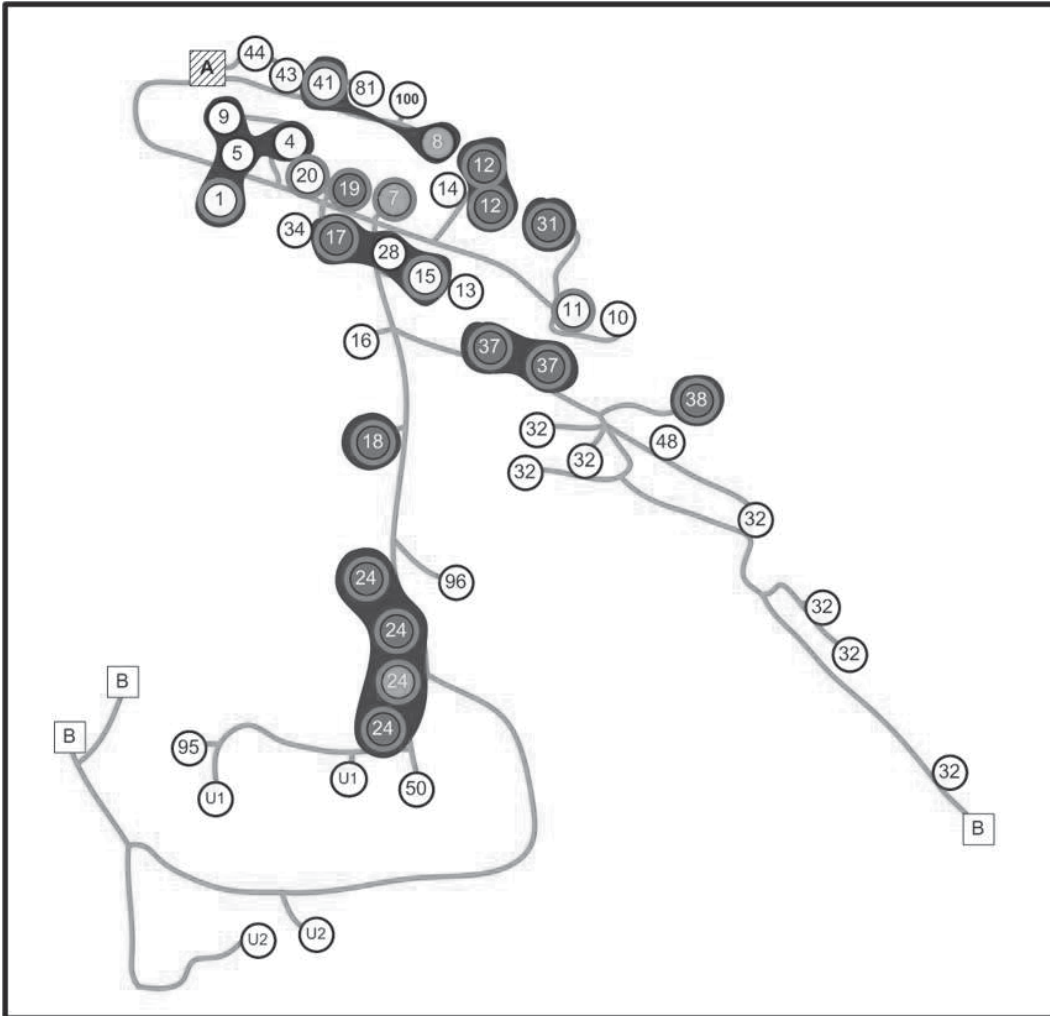


Figure 2.14: Clustering a Collection of Buildings with Local Generating Units based on Their Vicinity and Connectivity.

will lead a cluster. As shown on this figure, the light blue and red areas cover all no generators buildings. The remaining buildings in the light blue area will connect with the existing generators in the future, while there will be set a new generator in each red area. The small squares in between different microgrids represent the new remote-controllable switches. The distribution and the setting of the microgrids shown on the figure are based on the optimal operations and cost effectiveness. Figure 2.16 illustrates the separated microgrids with corresponding number, name, and the

generation capacity from Figure 2.15. We can treat each microgrid as one cluster. The capacity of each cluster is based on the estimation of energy consumption in the microgrid. Because there are no generators available in clusters 11, 12, and 13, the generation capacity of these three clusters are 0 kVA.

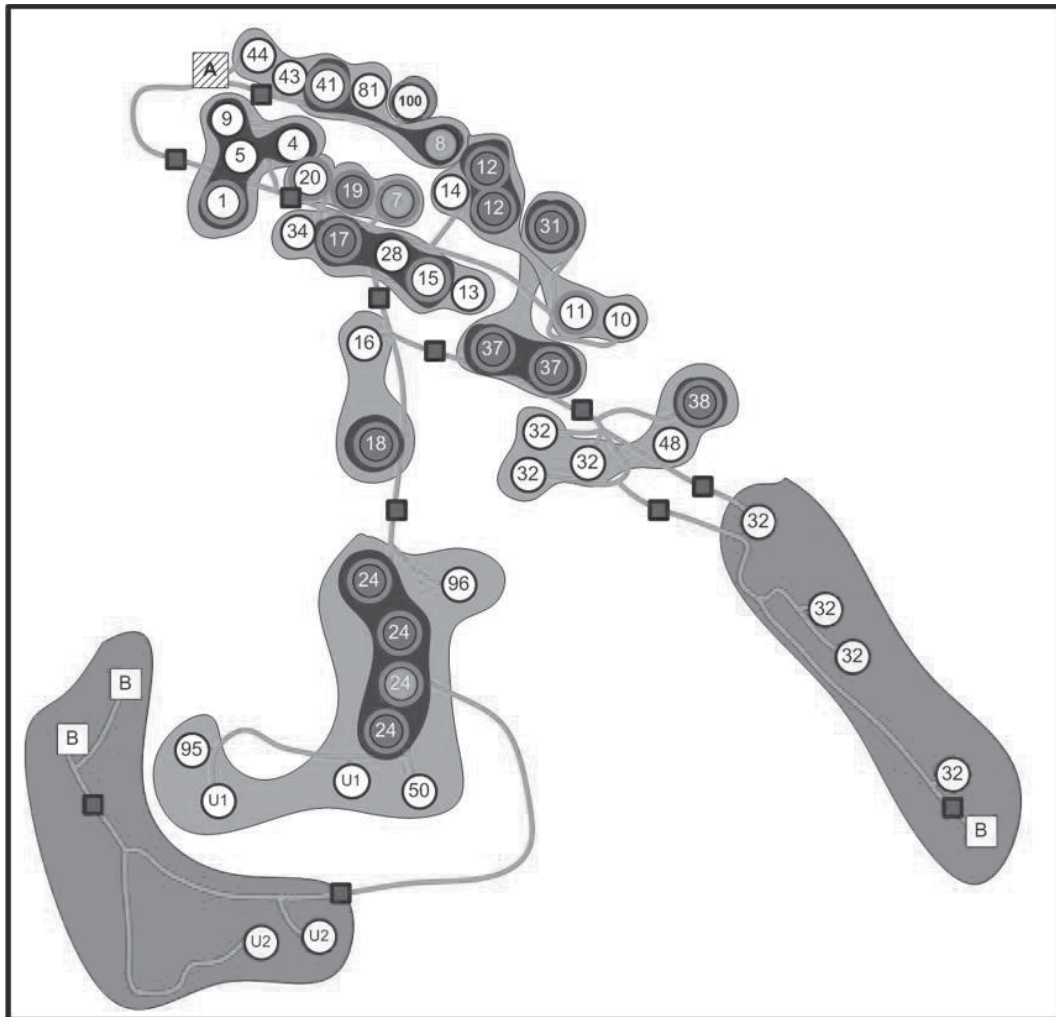


Figure 2.15: Potential Future Setup for a Networked Microgrid.

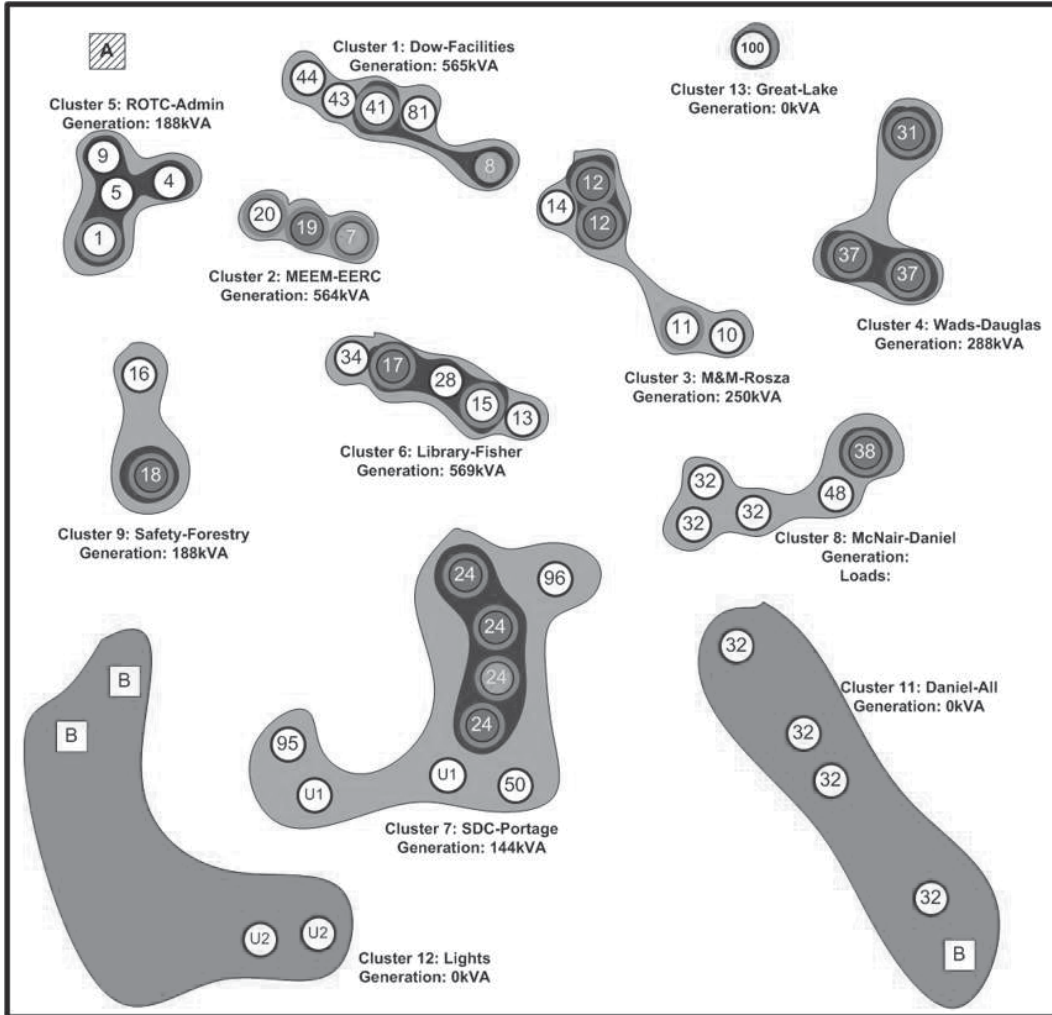


Figure 2.16: Cluster Numbering and its Total Capacity in kilo Voltage-Ampere (kVA).

Chapter 3

IMAGE EXTRACTION

ALGORITHM FOR

ELECTROMECHANICAL

ANALOG METERS

Increasing the number of metering points improves load observability. A higher rate of AMI deployment occurred between 2010 and 2011 due to the Recovery Act Smart Grid Investment Grant (SGIG) program [24] in addition to increased utility investments. However, there is not sufficient data to determine the level of smart meter penetration

beyond 2013. The IP-based electricity meter is the typical device used to collect real-time consumption data in secondary distribution systems [30]. Due to the pivotal role of information exchange between metering devices and the power distribution station, data observation and management of IP-based AMI are considered important roles in modernizing the distribution grid [36, 37].

Prevalent computing on mobile devices has revolutionized consumer electronic products and provided diverse applications in social networking. These devices are often embedded with powerful processors that can be utilized to perform relatively demanding tasks [38, 39]. Every new mobile unit comes with incremental features that can quickly become obsolete in the foreseeable future. The rapid pace of mobile device technology development results in a large secondary market of inexpensive devices with computing and imaging capability suitable for capturing and transmitting power consumption information from existing analog meters based on reasonable quality cameras. The contribution of this work is to establish a framework to perform real-time energy information extraction from images of the existing electromechanical analog meters.

3.1 Comparison between Three Different Metering Infrastructures

Different from IP-based meters, the electromechanical analogy meter is incapable of connecting with a network in any shape or form. Periodical human meter reading is the only method to acquire the accurate energy information from a concrete electrical building with mechanical meters. The electromechanical analogy meter uses four pointers with different orders of magnitudes to show energy consumption. To extend the working cycle of a meter, the displayed result should multiply a fixed parameter such as 400 or 800 and it is typically calibrated in kilowatt hours (kWh).

There are four different types of analog meters equipped in the distribution grid at Michigan Tech without data transmission performance. Type one is the meter denote consumption number with pointers, while type two shows numbers in a grey screen with detailed number information. Type three meter and type four meter are both capable of representing power usage values by digital numbers. The usage values on type three meters are shown on black screen with red laser number, while the other is on a blue screen with grey words, separately. The main difference between these two meters is the function of automatic display. Type four meter can only show data information by pushing relative buttons below the screen. Figure 3.1 below shows

these four types of analog and digital units that are not telemetered to the central control system.

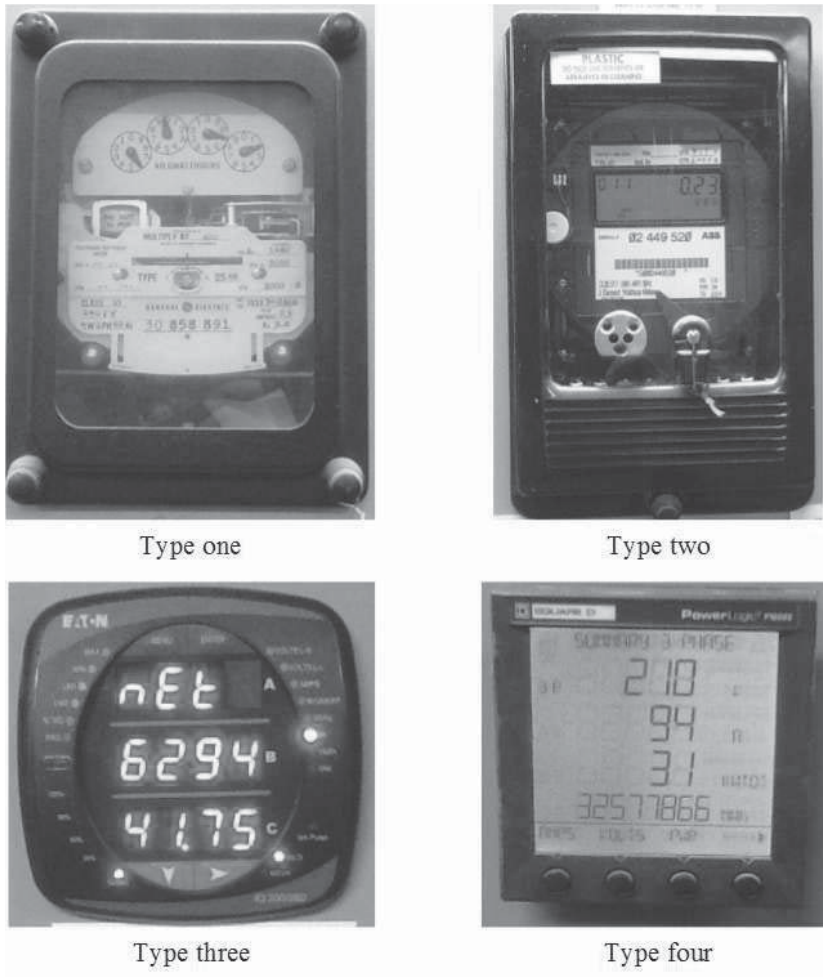


Figure 3.1: Four Types of Energy Meters for Campus Distribution Grid: Type 1: Analog with Pointers. Type 2: Analog without Pointer. Types 3 and 4: Non-telemetered Digital Meters.

Table 3.1
Comparison of utility costs between electromechanical meters, IP-based “smart” meters, and the IE approach.

	Electromechanical Meters	IP-based “Smart” Meters	Image Extraction Approach
Cost	Between \$30 and \$40 plus labor cost [40].	The estimated cost of a new meter is approximately \$80 [41]. Price largely ranges between \$200 and \$800 per circuit plus installation, management, and operating costs [41, 42].	Between \$100 and \$150 to consumers. Zero cost on labor as it is being installed by the consumer. Zero cost on the IT services as it utilizes existing Wi-Fi network.
Frequency of Data Collection	Once or twice every month, manually by crew team at site [43].	The interval can range between 10 to 30 minutes, depending on the utility’s preference. Data is sent to customer billing centers and being archived [44, 45].	The interval can be set between 5 to 30 minutes, depending on the utility. Data is sent to customer billing centers and archived.
Physical/Electronic Security	Physical perimeters are the setback due to energy thieves and malicious customers [46].	Prone to cybertampering. Malicious customers may alter the value of the energy consumption [41, 47].	May be prone to cybertampering. Utility would use security verification to accept or reject the acquired photos based on location and user account.
System Components	Electromechanical meters.	Smart meters, control panel, modem, and cables.	Timer camera device, device stand, wall charger.
Deployment Effort	De-energize the circuit and install the meter. Manhours would cost.	De-energize the circuit and install the meter. The technology may be obsolete and could be replaced with newer sensors [42, 44].	Does not require to de-energizing the circuit for installation. It is at consumer discretion whether they would participate in this program. Approval would be subject to security verification.
Data Flow	No data flow.	Open two-way communication, possibly with control variables [24].	One-way communication. Only kWh and kW information being sent.
Network Connections	Not required.	Wireless or wired connection [47].	Wireless connection.
Data Reliability	Not applicable.	Depend on home area network (HAN)/neighborhood area network (NAN) [48].	Depend on Internet availability at home by consumers.
Home Energy Management Real-Time Pricing Mode	Not available. Fixed price.	Metering and control modes [24]. Dynamic price [24].	Only metering mode. Fixed price.

Table 3.1 shows a comparison between: conventional electromechanical meters, IP-based “smart” meters, and the mobile device-based image extraction (IE) approach for the task of extracting kW and kWh information through mobile device.

The major differences between the methods are the frequency of obtaining the consumption data, equipment and installation costs, as well as data reliability and privacy. The low deployment and maintenance costs of the IE system are crucial for the sustainability of technological transfer of information between the electromechanical meters and the other two types. In addition, the IE approach may incentivize consumers to engage with utilities other than through bill payment. As most utility companies have databases that relate distribution transformers to the customers connected to them, power flow analysis could be updated with high frequency or on demand as needed in their distribution management system for more updated real-time calculations. Cybertampering can be a major concern, due to potentially malicious customers tampering or altering the metering values [49].

Although new “smart” meter devices provide an opportunity for consumers to reduce their monthly utility charges, utilities may not realize near-term profits from their use due to maintenance and installation costs. Hardware upgrade would affect the finance of new technology and the concern of cost recovery. In addition, some consumers may avoid “smart” meter installation due to concerns regarding the breadth of information it could be recording.

There are two major cost breakouts for an IP-based “smart” meter [42]. The total cost is approximately \$566 per device where it includes capital of the IP-based energy devices, as well as operation and maintenance. The “smart” meters would remain one of the expensive solutions in large-scale deployment. Currently, the utilities financial priority and governmental external funding opportunities are the constraints which leads to slower growth in term of the number of IP-based meters deployed. The cost does not include a complete upgrade of IP-based metering devices. Typically, technology changes every 5-10 years with higher performance and more sophisticated features that may improve the quality of consumption datasets.

Most mobile devices today are embedded with camera features, assisted GPS, and biometric sensor readers for user authentication purposes [50]. Mobile computing has significantly improved over the past few years where the tech-savvy consumers may utilize their older generation of devices for this purpose. If consumers decide to participate in a program on data collection, then it might help to increase the number of metering points within a distribution system. This active participation may increase the number of observable points in a shorter timeframe. As summarized in Table 1, these privacy and security parts remain a concern but can be further enhanced with biometric authentication. Many consumers upgrade their mobile devices on a two-year cycle with their old devices available for repurposing. Use of repurposed mobile devices means that the primary cost of the IE approach would be the mounting hardware with an estimated expense of \$140.

3.2 Campus Metering Testbed

The phase-one AMI deployment was commissioned at Michigan Tech can provide approximately half of the total campus power consumption and load information in real-time at an installation cost of \$60,000. A low-cost solution was desired to capture the remaining campus load with similar bandwidth. Although the upgraded infrastructure provides a high percentage coverage of system observability today, it may not in the future due to shifts in energy consumption as building usage changes. Thus, a flexible method for acquiring load information is desirable.

Within the campus Intranet, subnets of different buildings are connected and are routed through the campus-wide communication backbone network to other internal networks for real-time information sharing. This demonstration project is to increase a greater number of metering points for the lower priority buildings by deploying mobile devices that pictorially acquire energy information from existing electromechanical analog meters, instead of dedicated IP-based meters.

3.2.1 Design of Timer Camera

The design concept of real-time data extraction from the typical mechanical meter is to apply the live data transmission technology in cloud storage [51], which requires information upload to the private cloud space through campus Intranet and complete synchronization with the computer side. The pivotal component is the smart mobile device with a self-designed application to achieve time-lapse photograph and cloud sharing.

The achievement of the timer camera algorithm in programming language is not complicated. The first step is to call the command for the camera in the device. Of course, the accessory flashlight is also necessary especially in the dark environment. Then, we need to add a countdown timer before the camera calling command. The periodic timer can be set to capture pictures of the dial plate on electromechanical meter once every 900 seconds which is 15 minutes. Furthermore, we have to append a reset command at the end of the countdown timer to realize the automatic periodical pictures being captured. Taken photos will be directly saved in the photo albums and make sure the cloud photo sharing function is turned on.

The terminal console shows a series of photos taken from the mobile devices that show the time stamps when those were taken that can be approximated with reasonable

energy consumptions over certain period of time. The flowchart for the timer to take photo snapshots is shown in Figure 3.2.

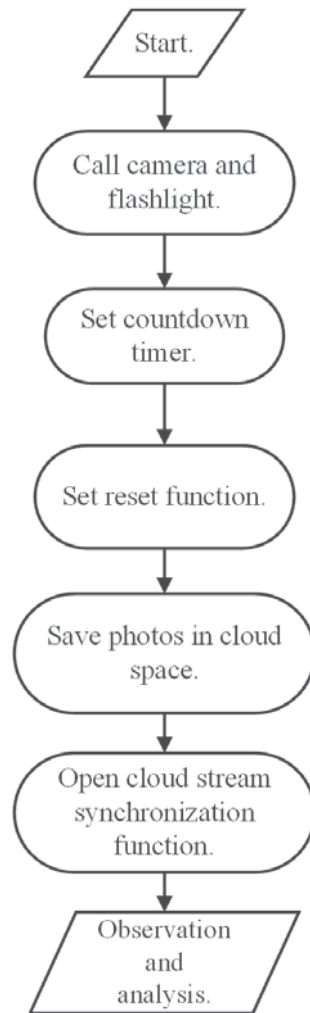


Figure 3.2: Flowchart of Timer Camera Design Algorithm.

3.2.2 Operational Mode of Mobile Devices

The mobile device with timer camera application should be placed in front of the dial plate with a stand support. The location selected should be under Wi-Fi coverage

to ensure the continuity of data transmission. A better way to improve the quality of transmission is to make sure there is sufficient data traffic for each device, which means turning off other functions or applications in the mobile device during the image acquiring procedure. In addition, the test place should have power outlets to provide continuous power supply. The cloud-sync photo will appear at the data monitoring terminal immediately [52] and ready for image extraction. The operating process of mobile devices transfer pictorial data through wireless networks demonstrated in Figure 3.3. This process is to gather close-to-real-time power observation to model the loads for the remainder of unmetered buildings.

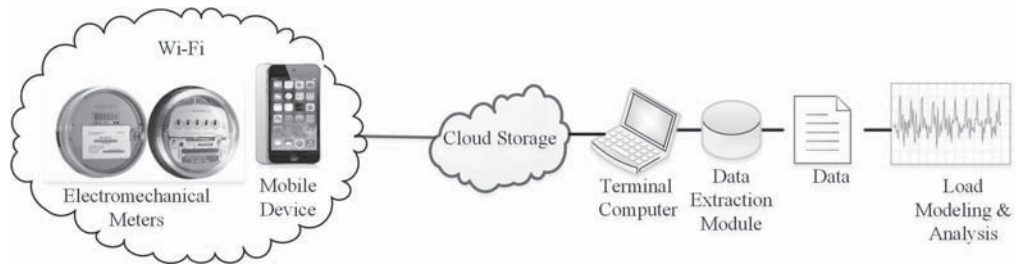


Figure 3.3: Image Snapshots to the Cloud with Key Processing Elements.

Figure. 3.4 depicts the overall framework of real-time data acquiring procedure which includes mobile devices transfer pictorial data between wireless networks and the basic architecture of the AX supervisor. The proposed framework transfers the image data to a centralized database. Within the existing system, the IP-based meter data are monitored with a web supervisor and browser through specific virtual private network access and then saved to the campus data server. The proposed framework uses two-way communication which means a one-side transmission delay would cause delay of image transfer to the cloud. Reliability can be increased if there exists a Long-Term

Evolution (LTE) network in addition to the Wi-Fi connection. This assumes the repurposed devices are LTE enabled. Both reliability and latency can be negatively impacted if there is poor wireless reception, which often increases with the distance between the mobile device and the hotspot. Additional communication latencies are introduced (i) between the device and the cloud, and (ii) between the cloud and the data center of the server performing the data extraction. In our experiments, the total latency was always less than one minute. As described later, test results showed a maximum delay of one minute. The main threat of IE approach is that the availability of wireless connections could sometimes be abruptly disconnected.

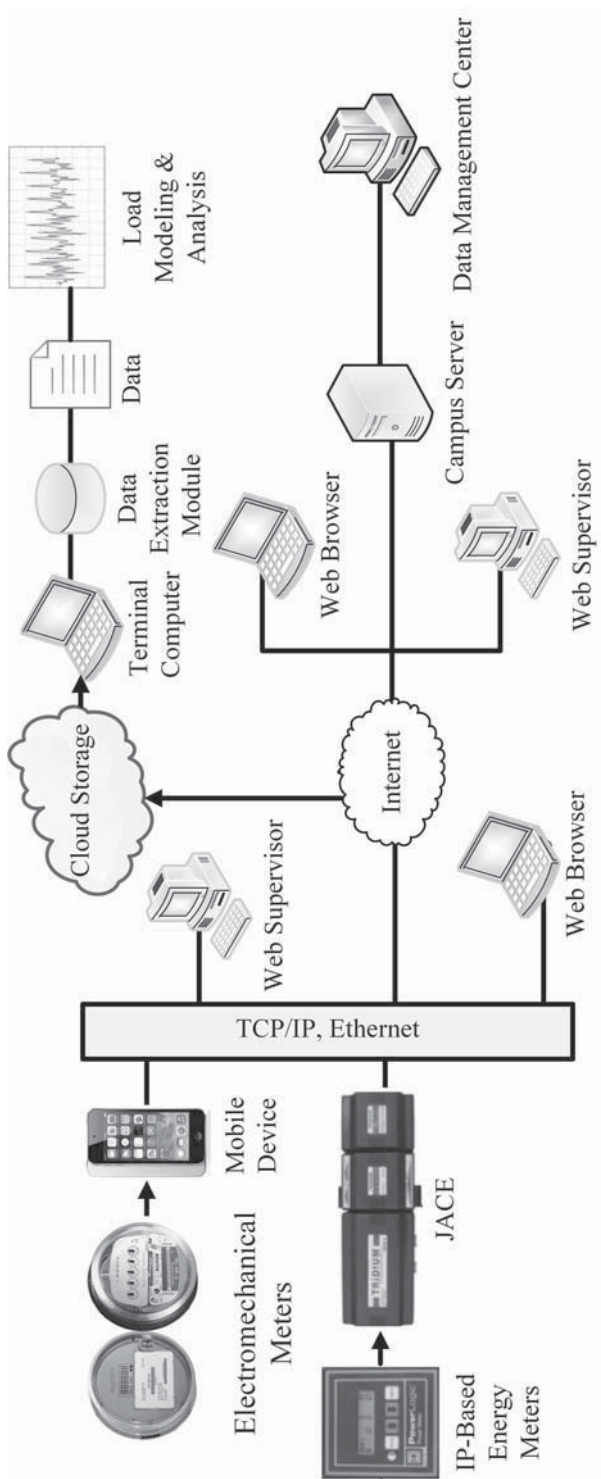


Figure 3.4: Metering Infrastructure for Campus Distribution Grid.

3.2.3 Pictorial Data from Electromechanical Meters

Unlike IP-based “smart” meters, the electromechanical analog meters do not establish network connection and require periodic manual reading. The typical analog meter has four pointers with different orders of magnitude to show scaled energy consumption.

The overall approach for real-time data extraction from the typical mechanical meters is to apply live image transmission technology with the information uploaded to a private cloud storage [51] through the campus Intranet with synchronization achieved at the terminal computer. The operational approach is to have a mobile device with a timer camera application acquiring images every c minutes.

The automatic upload function in the mobile device uploads the photo stream to the private cloud through the Internet and then the photo appears at the monitoring terminal computer immediately for image processing and the consumption data extracting process [52].

Data samples of the IP-instrumented buildings were used to find a suitable value of c ; trading off frequency resolution, and phase lag with the size of datasets. Figure. 3.5 is an example that illustrates the average values of time-activity curves of sample data acquired from an IP-based meter with three different time durations. According to the

purposed simulated visualization, we can estimate future power consumption during the same time period to realize efficient power control and supply. The estimated power in kW is determined based on a first-order finite difference of the two image snapshots.

$$P_{est} = \frac{E_{mec}(t) - E_{mec}(t - 1)}{c} \quad (3.1)$$

According to the equation 3.1, $E_{mec}(t)$ and $E_{mec}(t - 1)$ are the latest image snapshots of the electromechanical analog meter. If we restrict the interval to be every 10 minutes, then $c = \frac{1}{6}$ using an hourly base.

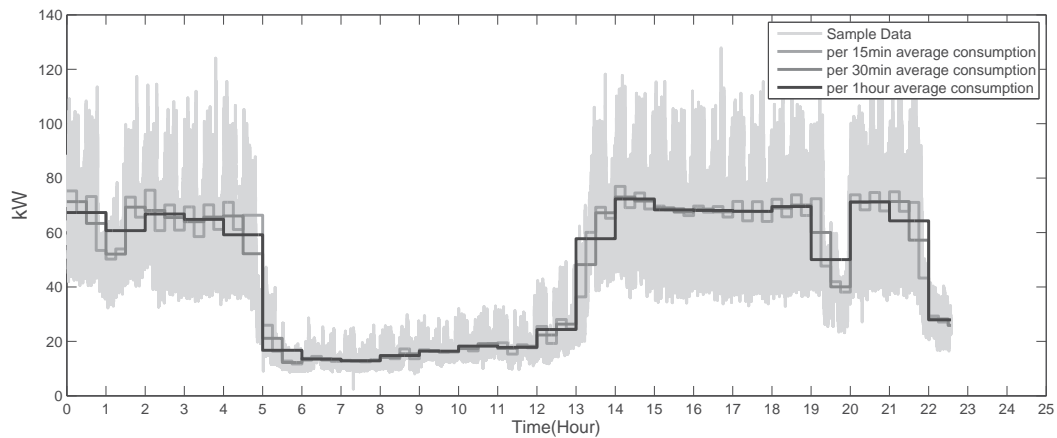


Figure 3.5: Proposed Simulation of Energy Consumption Using Sample Data.

3.3 Data Extraction from Snapshot Images

The real-time data acquired from existing electromechanical analog meters is implemented to improve the observability of campus distribution grid without deploying expensive IP-based wired meters. These mobile devices which are connected through Wi-Fi to the cloud will provide real-time snapshots of operating states together with the other 11 buildings containing IP-based meters. This reveals energy data variation within a specific time period. Within a limited time duration, the curve illustrates that the demanded quantity of energy consumption can be utilized to forecast or adjust the system consumption as part of the studies. The trending information from these devices is compared in order to generate common time-activity curves across all metered buildings.

3.3.1 Data Extraction for Electromechanical Analog Meters

3.3.1.1 Image Segmentationn

The serviceable portions in the original image of the traditional mechanical meter shown in Figure 3.6 (a) are the four dial plates. For the consideration of processing time and identification effect, the idea here is to discard useless sections and keep

the indispensable rectangle illustrated in Figure 3.6 (b) that contains all four dial plates, based on the notion of image matrix segmentation. The automatic pointer reading algorithm aims at an individual dial plate, which we need to separate the extracted rectangle shown in Figure 3.6 (b) which then needs to be divided into four squares that dial plates embedded as shown in Figure 3.6 (c). Due to the fact that the original shape of a recognized target is a standard circle, we can set the center of each square as the circle's center and half of the side of each square as the radius to the corresponding circle. As a result, the four inscribed circles shown in Figure 3.6 (d) are the object that we will perform further analysis upon.

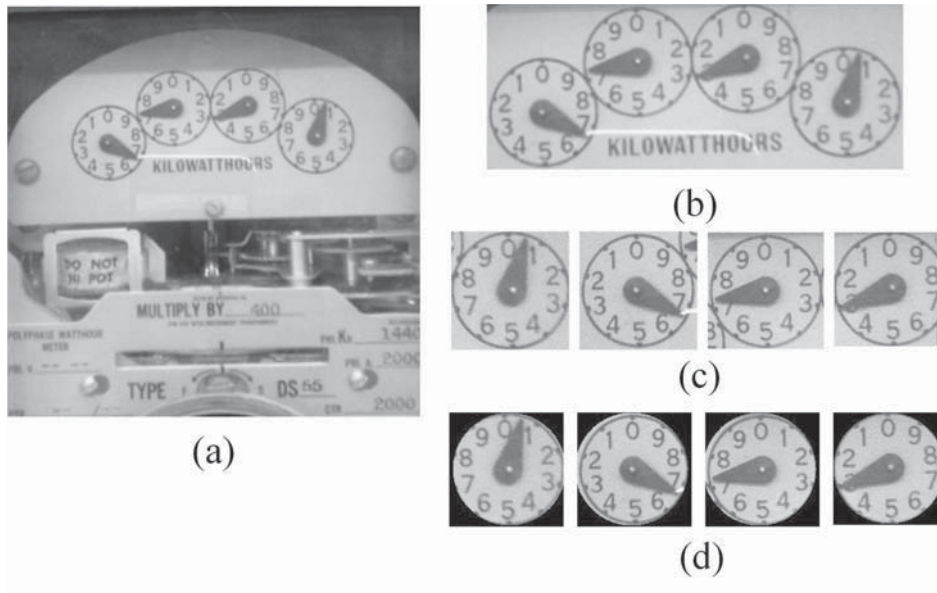


Figure 3.6: Image Segmentation in 4 Steps from (a) to (d).

3.3.1.2 Digital Image Preprocessing

The change in light conditions can lead to color and contrast variance in the hand of the dial. In order to avoid the identification error generated from this situation, the first step is to produce parallel grayscale images from segmented targets. Discerning grayscale images directly is often accompanied by random noise as well as diverse shade degree in the reorganization zone of images. Here, we utilize grayscale image binarization to acquire analyzable outcomes with little identification error. It should be noted that the threshold value of binarization should be 0.6, which is larger than the default value 0.5 to magnify the contrast ratio of white objects.

In addition, to improve resolution in the binary image, we apply specific mathematical morphological operations to simplify the image initial data structure without changing the basic configuration. These optimized operations are mainly based on dilating and corroding [53]. The dilating operation expands and enhances the edge of the object to dislodge or cover blank spots around object edges while the corroding operation eliminates external pixels of object to reject “burrs” in edges. Dilating and corroding smoothes the surface of objects.

Removing the H-connected element in the object applies the concept of dilating [53]. The edges of two objects in an image are connected by splashes during the process of binarization. A scattered point connecting two edges is considered as an H-connection.

To separate these two independent objects and generate the image, we need to remove all unnecessary pixels. The operation of this procedure can be shown using an example binary matrix:

$$\begin{pmatrix} 1 & 1 & 1 & 1 \\ 0 & 1 & 0 & 0 \\ 0 & 1 & 0 & 0 \\ 1 & 1 & 1 & 1 \end{pmatrix} \quad (3.2)$$

which then becomes

$$\begin{pmatrix} 1 & 1 & 1 & 1 \\ 0 & 0 & 0 & 0 \\ 0 & 0 & 0 & 0 \\ 1 & 1 & 1 & 1 \end{pmatrix} \quad (3.3)$$

Two rows of sequential pixels are connected by two slashes to construct an H-connection in matrix 3.2. After the removing process, the H-connection is broken and the two scattered points are eliminated in matrix 3.3.

The spur pixel is the redundant point or small branch that connects with the smooth edges of a object that can be considered as a fraction of the rough edges of a neat object. The process of deleting spur pixels is similar as corroding [53] that removes end points of lines without removing small objects completely. The implementation

procedure can also be described with a simple binary matrix example:

$$\begin{pmatrix} 0 & 0 & 0 & 0 \\ 1 & 1 & 1 & 0 \\ 1 & 1 & 0 & 0 \\ 1 & 1 & 0 & 0 \end{pmatrix} \quad (3.4)$$

which then becomes

$$\begin{pmatrix} 0 & 0 & 0 & 0 \\ 1 & 1 & 0 & 0 \\ 1 & 1 & 0 & 0 \\ 1 & 1 & 0 & 0 \end{pmatrix} \quad (3.5)$$

As shown in matrix 3.4, there is a spur pixel in the third column. In order to obtain the objective result, disposing should eliminate the redundant point to transfer the original matrix to matrix 3.5.

The inverted image is shown in Figure 3.7 and is ready for pointer extracting.



Figure 3.7: Exported Images After Segmentation and Preprocessing.

3.3.1.3 Pointer Extraction Algorithm

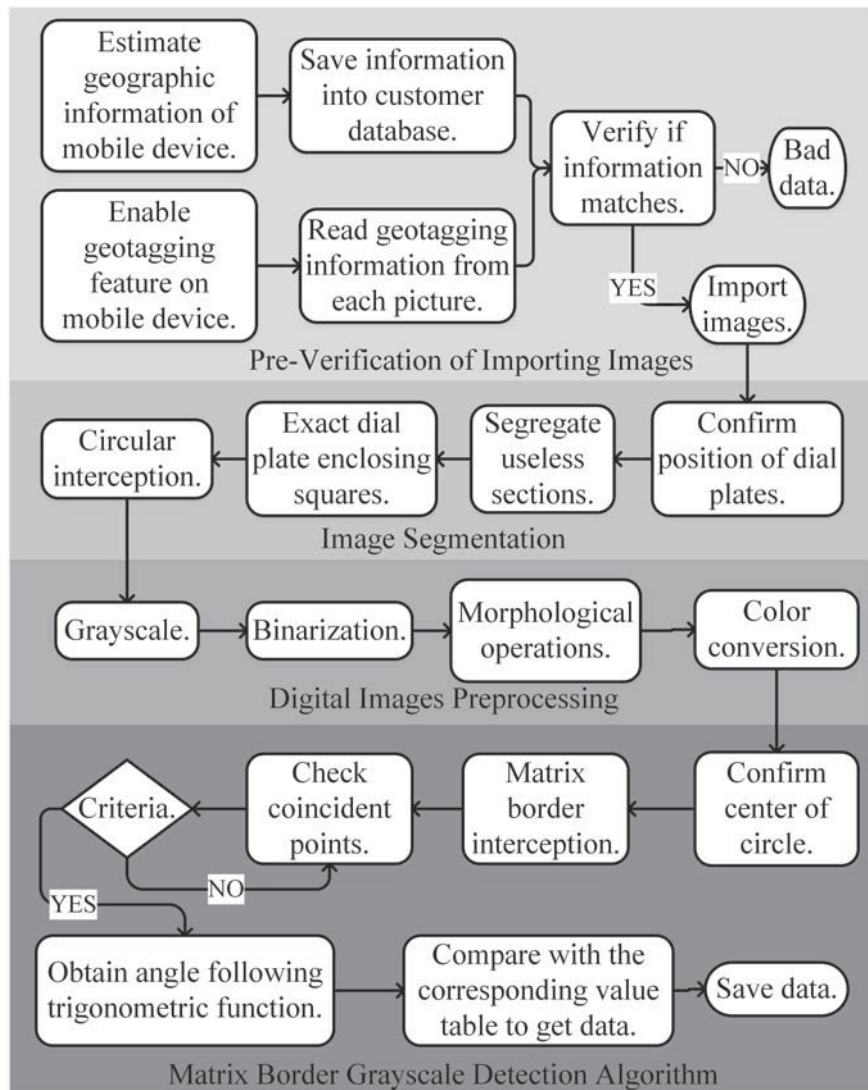


Figure 3.8: Flowchart of Matrix Border Grayscale Detection Algorithm.

Figure 3.8 demonstrates the flowchart of the overview process of image data that is extracted from pointer analog meters. The image data is transferred between mobile devices and the cloud. This is presumed to be sent from consumers to the cloud, and then the data transfer between cloud and customer billing center. The flowchart

includes security verification, which includes following steps:

1. Estimated latitude and longitude position of the mobile device based on Wi-Fi or assisted GPS information.
2. Each photo taken has the geotagging information that consists of latitude and longitude. The geotagging feature has to be enabled on the mobile device.
3. Images are transferred to the database of customer billing center. Before the data extraction begins, the geotagging information is verified together with the username and address of the customer's database.
4. If they matched, then the data extraction algorithm starts processing. If some images violate the criteria that is expected, then those will be disregarded and the data points will be indicated as bad ones and the result not to be considered.

An AMI system is expected to last between 15 and 20 years, while the life cycle of proposed IE approach could vary significantly based on the device used. Similarly, the IE cost is also highly variable depending on the availability of repurposed devices. The time interval setting of transmitting the image datasets was set to be every 10 to 15 minutes. The Internet today has the bandwidth sending pictures through Wi-Fi. Furthermore, the geotagging features from assisted GPS devices only shows the location of the device rather than the position of the customer (since this is a repurposed unit). These pictorial datasets do not include the name of the customer

or their billing information.

Digital images stored on computer memory in bitmap format use a rectangular lattice. In the dot matrix, each point is a pixel. Generally speaking, values of gray pixels are divided into 256 scales: from the black color as 0 to the white color as 255 [54]. A colorful picture with the size of $m \times n$ is equivalent to $m \times n$ pixels with diverse gray values, but a binary image only contains black and white pixels. Our pointer extraction algorithm is based on the characteristics of the binary image matrix and is designed to intercept a square border within an image as illustrated in Figure 3.9. The angle Θ is found by superimposing a square onto the extracted image as shown in Figure 3.9. The first and last intersections of the square with the boundaries of the pointer pixels are used to find the pointer's midpoint, also indicated on Figure 3.9. Finally, the pointer's angle is computed by the line segment connecting the circle center to the pointer midpoint.

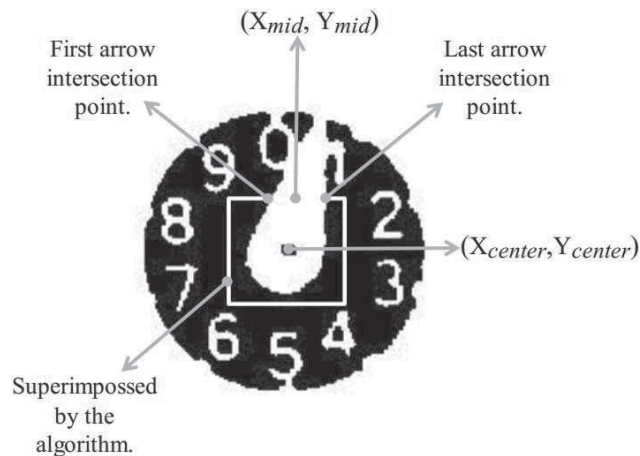


Figure 3.9: Intercepted Square Box with a Dial Plate Arrow within an Image.

When traversing the square to find the pointer intersection points sometimes spurious pixels are found that can give a false positive intersection. These are filtered out if their surrounding pixels are inverted. Depending on the midpoint and the center of a circle, the offset angle, Θ , is calculated based on the pointer position in each quadrant using the appropriate quadrant dependent version of Equation 3.6, where X_{mid} , Y_{mid} and X_{center} , Y_{center} present the coordinate of the midpoint and center of the circle, respectively.

The goal of the pointer extraction algorithm is to find the value, d , indicated by the pointer. This is accomplished by first finding the angle the pointer makes with the dial plate, Θ , and then using Equation. 3.7. For the fastest moving dial (most right) the resolution of the algorithm is 3.6° , which indicates n is equal to 2. For the first three dial plates, the accuracy is in integer bits and the n should be equal to 1. Under certain circumstances, the adjacent pointers on electromechanical analog meters may have an inverse numerical plate, i.e., clockwise and counter-clockwise, in (3.7).

$$\Theta = \begin{cases} \tan^{-1} \left(\frac{|X_{mid}-X_{center}|}{|Y_{mid}-Y_{center}|} \right) + \theta_0, & \theta_0 = \begin{cases} 0, \text{ quadrant 1} \\ \pi, \text{ quadrant 3} \end{cases} \\ \tan^{-1} \left(\frac{|Y_{mid}-Y_{center}|}{|X_{mid}-X_{center}|} \right) + \theta_0, & \theta_0 = \begin{cases} \frac{3\pi}{2}, \text{ quadrant 2} \\ \frac{\pi}{2}, \text{ quadrant 4} \end{cases} \end{cases} \quad (3.6)$$

$$d = \begin{cases} \text{trunc}(\Theta/(2\pi/10^n)), & \text{clockwise} \\ 9 - \text{trunc}(\Theta/(2\pi/10^n)), & \text{anticlockwise} \end{cases} \quad (3.7)$$

3.3.2 Data Extraction for Energy Meters with Digital Unit Display

In this section, we present the procedure how to extract the digital display from the panel which also includes the image processing and image segmentation. The algorithm will also be described in this section.

3.3.2.1 Digital Images Processing

Digital image processing is introduced here to systematically convert the pictorial information into a binary number with two major steps, i.e., (1) conversion from color picture to grayscale, and (2) binarization. As mentioned, the binarization is a process to convert the original image into binary with more than 200 values indicating near white color and zeros for black color. For the purpose of contracting the image with black and white color, the threshold value has been set to 0.5 as its default instead of 0.6. The threshold value with 0.6 was originally used for the pointer of the analog images.

3.3.2.2 Image Segmentation

Figure 3.10 (a) shows the image of automatic display number analog meter. After grayscale processing, we could acquire Figure 3.10 (b). For the consideration of processing area, a rectangle portion of the image is cropped, which is shown in Figure 3.10 (c). Then, the inverting corresponding binary version processing area is illustrated in Figure 3.10 (d). The top number on the dial plate represents the energy consumption data, which is the only data we are concerned with. Dividing this number string into four independent numbers within four rectangles with the same height and width. Figure 3.10 (e) shows the four objects will be further analyzed.

3.3.2.3 Comparison Algorithm for Pixel Differences

Same as the matrix border grayscale detection algorithm, the pixel differences comparison algorithm is also based on pixel analysis. The idea of his algorithm is relative to the former one and the binary analyzable object only contains black and white pixels.

First, we collect a numerical range for each object, which means we capture all numbers from 0 to 9 for all the four positions. Then, we save them as four independent number libraries after acquiring the four inverting binary objects. After that, we



Figure 3.10: Digital Images Preprocessing and Image Segmentation in 5 Steps: (a) Original Image. (b) Grayscale Image. (c) Binarization Outcome. (d) Counter-color Outcome. (e) Analyzable Objects.

compare the pixels differences of the new pending images in each position with the saved number libraries. The four numbers shown on each position with minimum pixel differences are the final results we prefer to obtain. Figure 3.11 demonstrates the overview flowchart of the pixel differences comparison algorithm.

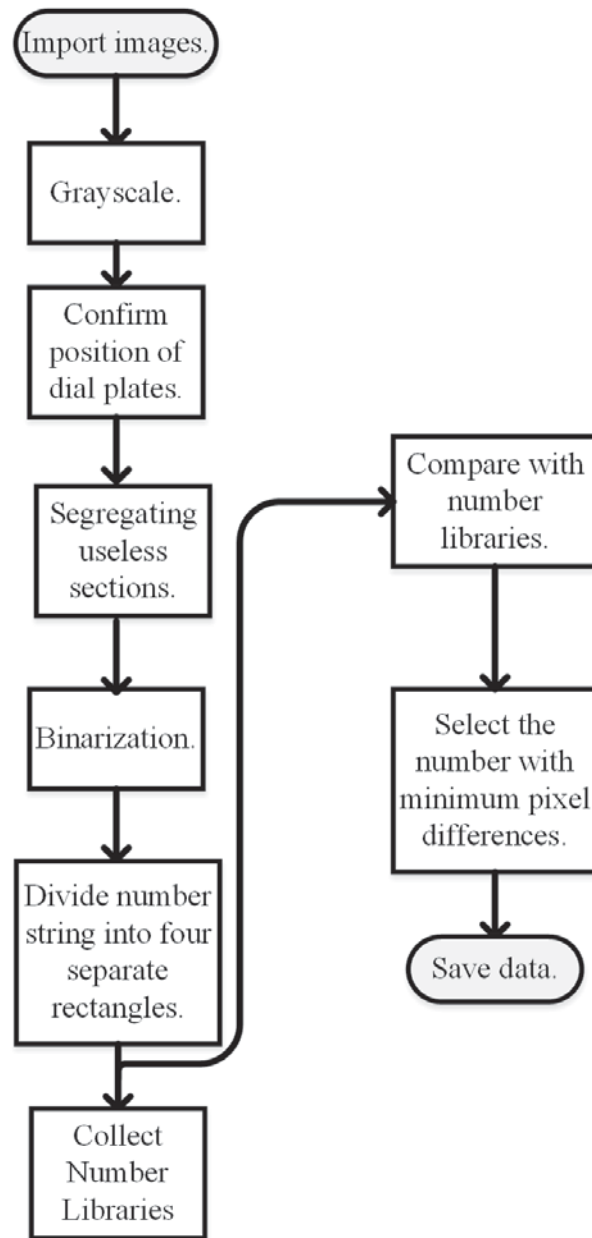


Figure 3.11: Flowchart of Pixel Differences Comparison Algorithm.

Chapter 4

CASE STUDY

The image extraction (IE) approach was validated on a test case using the existing electromechanical meters in a building connected to part of the Michigan Tech distribution system. The evaluation of time-activity curves is discussed in this section.

4.1 Decision to Select an Unmetered Building

In order to prove the proposed method can be simulated and validated using the existing analog meters in remaining buildings, we should confirm at least three conditions: what type of meters are in the objective building, does Wi-Fi cover this area, and is there a power outlet to provide continuous power for simulation device. We

process a statistical survey for remaining buildings and complete the two forms shown in Figures 4.1 and 4.2.

NUM	Name	Type 1	Type 2	Type 3	Type 4
1	Administration				
4	ROTC Building				
5	Academic Offices				
6	ANNEX Building				
10	Rozsa Center				
11	Walker Arts and Humanities Center				
14	Grover C.Dillman Hall				
15	Fisher Hall				
20	Mechanical Eng. & Eng. Mechanics				
28	Rekhi Hall				
32	Daniel Heights				
34	Memorial Union Building				
41	Central Heating Plant				
43	Ground Maintenance				
48	Hillside Hall				
81	Power Generation Building				
95	Advanced Technology Center				
96	Portage Health Center				
100	Great Lakes Lab				
U#1	SDC Parking Lot				
U#1	SDC Lights				
U#2	Football Stadium				
U#2	Sharon Ave.				

Figure 4.1: Four Types of the Remaining Unmetered Buildings.

The statistical tables demonstrate most of the remaining buildings equipped with type one electromechanical meters. There are only three type two meters even though six buildings use this type of meter because some buildings share one meter to measure the amount of electricity consumption. We mentioned the automatic reading algorithm of the type three meter, but there are only two type three meters on campus.

NUM	Name	Comment	Wifi	Outlet
1	Administration	In box, hard to read	NO	NO
4	ROTC Building	Combine with Building 5	YES	YES
5	Academic Offices	Combine with Building 4	YES	YES
6	ANNEX Building		YES	YES
10	Rozsa Center	Combine with Building 11	NO	YES
11	Walker Arts and Humanities Center	Combine with Building 10	NO	YES
14	Grover C.Dillman Hall		NO	NO
15	Fisher Hall		NO	YES
20	Mechanical Eng. & Eng. Mechanics	One 208/Two 480	YES	YES
28	Rekhi Hall	Not clear/Push buttons	YES	YES
32	Daniel Heights	Outside/3 or 4 show in one meter	NO	NO
34	Memorial Union Building		NO	NO
41	Central Heating Plant	Two types meters	YES	YES
43	Ground Maintenance	Combine with Building 41	YES	YES
48	Hillside Hall		YES	YES
81	Power Generation Building	Combine with Building 41	YES	YES
95	Advanced Technology Center	Show one value without push buttons	NO	NO
96	Portage Health Center	Outside	NO	NO
100	Great Lakes Lab		NO	YES
U#2	Football Stadium	Outside	NO	NO
U#1	SDC Parking Lot	Outside/Combine with building 96	NO	NO
U#2	Sharon Ave.	Outside/Combine with building 96	NO	NO
U#1	SDC Lights	Outside	NO	NO

Figure 4.2: Wi-Fi and Outlet Availability for Unmetered Buildings.

Building 95 has type three meter (not telemetered) but it is not electrically connected to the campus distribution grid. The other type three meter is installed in the Hillside Hall (building 48) that has the local archive, which is also not telemetered to the central heating plant (CHP) database. However, this building has already achieved real-time data monitoring even though its data can only be shown on the local archive. To consider as part of the selection, the buildings that do not meet those two criteria are not studied. The proposed extraction algorithm on electromechanical analog meters with pointers can be used for the case study here.

4.2 Test Case Setup

As shown in Chapter 2, Figure 2.1 shows the geographical map of the campus distribution network with numbered buildings. The proposed IE system was tested in the unmetered building 20, which is the Mechanical Engineering and Engineering Mechanics building (MEEM). This building was selected because of its relatively high consumption relative to the other unmetered buildings and based on the additional criteria considered for the study are to ensure that the location is equipped with outlets and Wi-Fi availability. Building 20 had all of them. As the 120V supply near a meter is pretty rare, a power cord is necessary to connect the wall outlet with the device charger. In addition, the implementation of the proposed framework was secured in the electrical room of building 20 and thus weather protection of the device was not considered.

Two different types of electromechanical analog meters were present in MEEM electrical room: 208-V and 480-V. The 208-V meter monitors low power-driven equipment such as lighting and electronic locks while the 480-V meter detects high-power machinery loads. The case study was based on both meters, and the datasets obtained from meter readings were recorded for nine days.

Two IE systems were deployed with the timer-camera application placed in front of

the dial plates as shown in Figure 4.3. The captured images were automatically and wirelessly uploaded to the server every 15 minutes and were also displayed on an attached computer. The umbilical shown in the figure was for power only.



Figure 4.3: Actual Timer Camera Device in Operational Mode.

It should be noted here that the stored name format of the electromechanical meter photo in cloud storage is the title “IMG” with a serial number, e.g. IMG_1110. There are two methods to import a series of photos captured during a time duration into the image data extracting program. The first is to utilize photo renamed software like “Photo Cap” to rename each one as a digital form. An alternative process is to utilize the programming functions to convert unidentified names into characters strings, i.e., “strcat” command in Matlab or C language.

4.3 Study Results

Converted meter readings were saved in a text file for subsequent analysis. The change in power usage, extracted from the 15-minute sampled images and averaged to hour increments, is shown in Figures 4.4 and 4.5 for both the 208-V and 480-V circuits. The curve of the actual data from the 208-V circuit is similar to a bar chart rather than the typical line chart because the energy consumption variability of the low power devices was small between 15-minute updates.

From equation 3.1, the energy information (in kWh) on those analog meters can be translated into average power (in kW). As the rotation of the electromechanical blade can be slow (scale of 800), considering the time-activity curves of average consumption with 15-minute, 30-minute, and an-hour timescale can help to estimate and predict energy consumption over a longer period of time. The initial outcome of the datasets is shown in Figures 4.6 and 4.7 which demonstrate the power estimates averaged at three different time intervals. This illustrates the ability of the IE approach to produce the trends of energy usage over time.

Table 4.1 illustrates the error rate analysis between the IE approach and manual reading. Four time intervals for 1 day, 2 days, 5 days, and 7 days are shown and corresponds to the range of dates 3/22/2014–3/23/2014, 3/22/2014–3/24/2014,

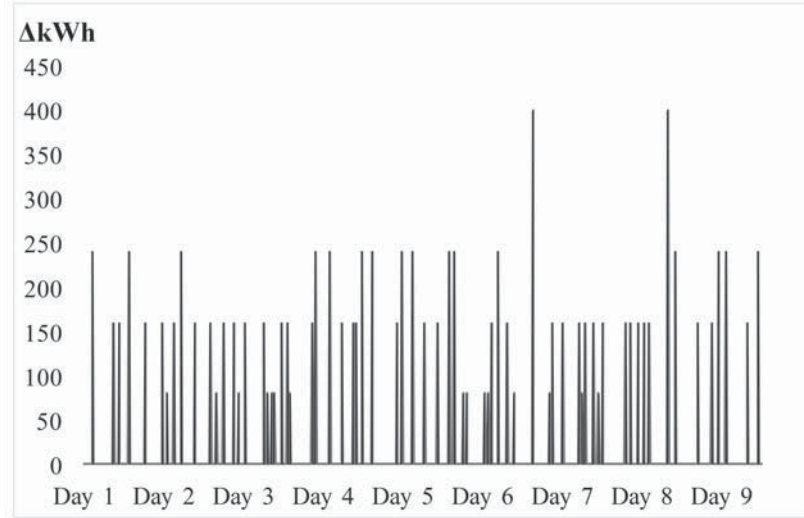


Figure 4.4: Energy Consumption of Building-20 208-V Circuit Between March 22, 2014 and March 30, 2014.

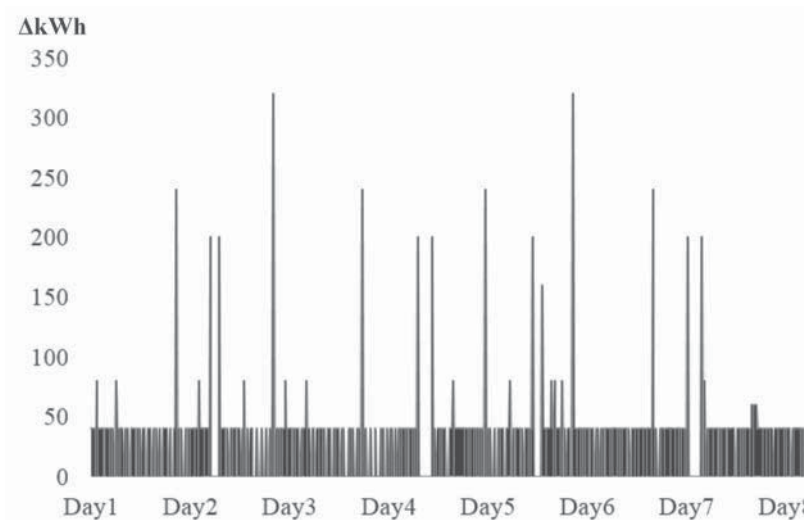


Figure 4.5: Energy Consumption of Building-20 480-V Circuit Between March 22, 2014 and March 29, 2014.

3/22/2014–3/27/2014, and 3/22/2014–3/29/2014. Since the manual reading time stamp was 6:00 pm (+/- 5 minutes), the nearest IE time stamp of 6:06 pm was chosen. The error between the IE approach and manual reading was always less than 0.5%.

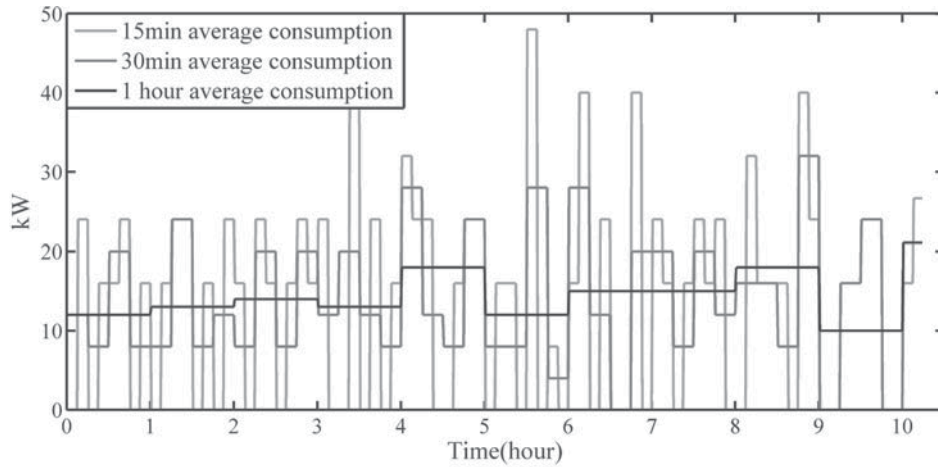


Figure 4.6: Average Consumption for Building-20 208-V Circuit.

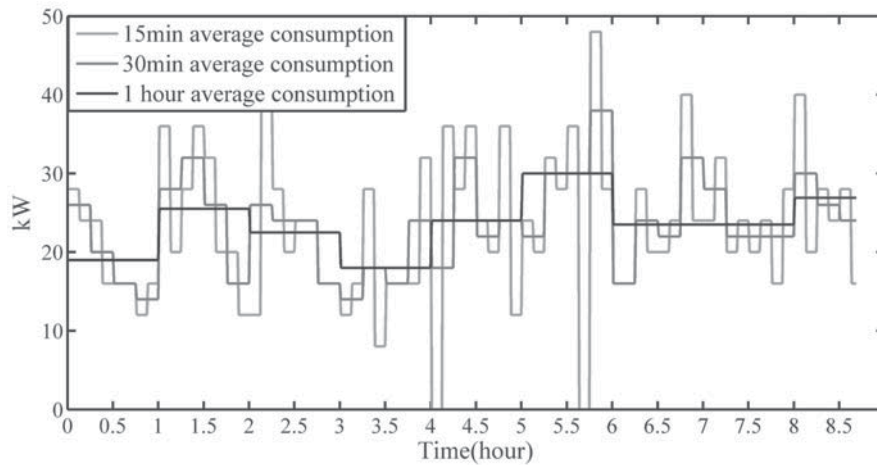


Figure 4.7: Average Consumption for Building-20 480-V Circuit.

Table 4.1
Error rate analysis

Number of days	Image taken time stamp	IE approach (kWh)	Manual reading timestamp	Actual consumption (kWh)	Error rate (%)
1	6:06pm	3,440	6:00pm	3,431	0.26
2	6:06pm	6,920	6:00pm	6,888	0.46
5	6:06pm	17,240	6:00pm	17,189	0.30
7	6:06pm	24,220	6:00pm	24,134	0.36

In addition to using the IE approach for continuous monitoring, it can also be used for determining which buildings should be targeted for more sophisticated instrumentation deployment. Fig. 4.8 compares the IE-based penetration on the total campus consumption with respect to the ten buildings smart meters and the rest of the unmetered buildings. Time intervals of 6 h, 12 h, 1 d, 2 d, 5 d, and 7 d are shown.

Building 20's consumption (labeled "Proposed Method" in the figure) is approximately 3.5% of the total (35 buildings) throughout the 6 time intervals from March 22, 2014 to April 1, 2014. In March 2014, the monthly consumption percentage of building 20 is with the average values of 3.51%. This consistently indicates the estimation of energy consumption from the unmonitored building via the IE system is reasonable. The energy consumption of building 20 is apparently higher than the average consumption of each of the 25 unmetered buildings (labeled as "Analog Meters"), which are the campus insignificant loads.

The statistics of the AMI are the accumulation values that sum up all 10 buildings with smart meters. About one-fourth of the total consumptions, which is the remainder of the 25 buildings, does not have smart meters nor implemented with the IE approach. Through the observation of those 6 piecharts, the proportion of energy usage on those 10-building smart meters is estimated to be about 70 percent of total campus consumption, which is considered the heavy loads of campus.

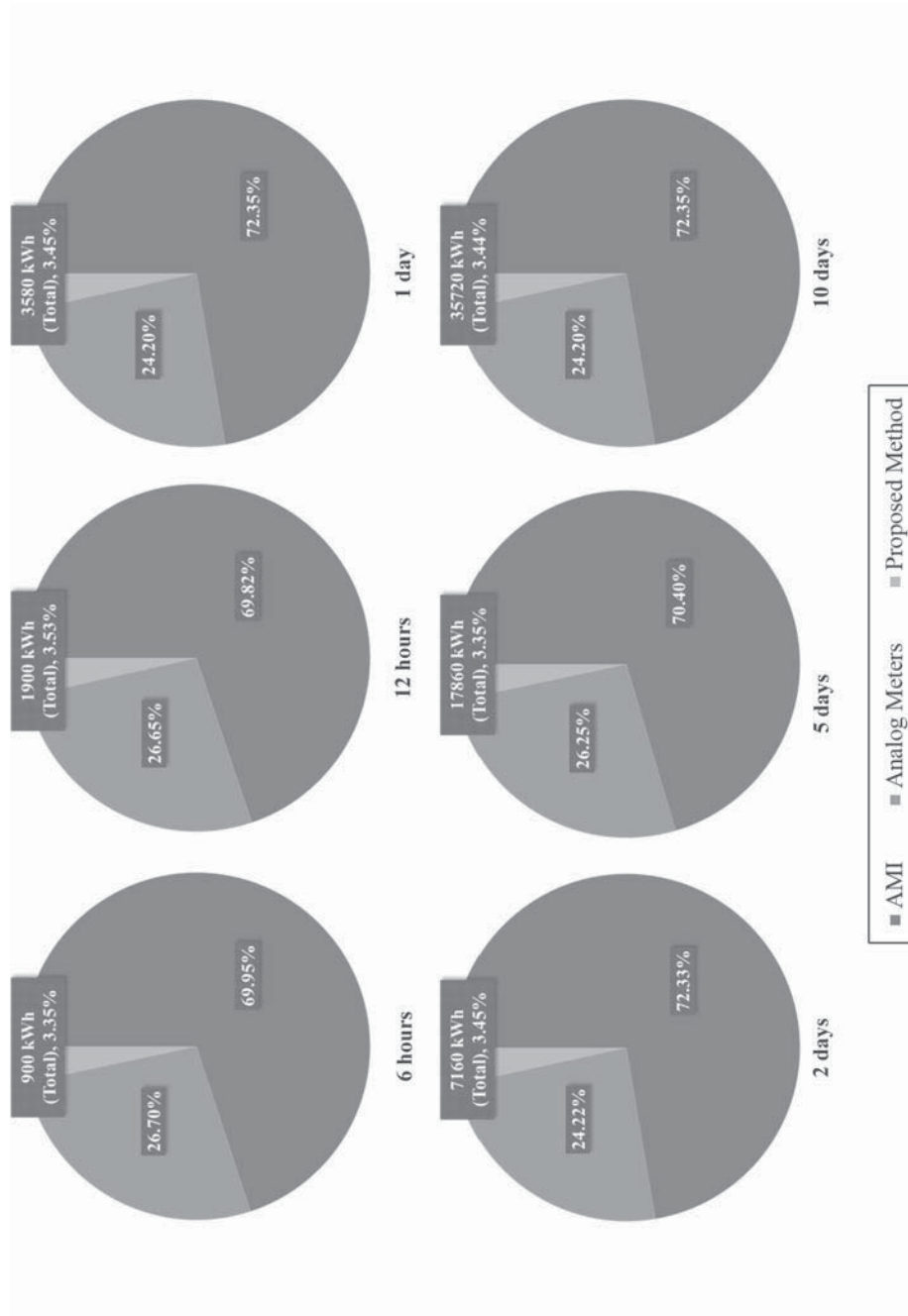


Figure 4.8: Consumption Percentage Piecharts for Buildings with AMI, Analog Meters, and Analog Meters with Proposed Method (Number 20).

Chapter 5

CONCLUSION AND FUTURE WORK

Along with the evolution of information communication technology, the labor-intensive meter reading has been replaced gradually by the IP-based metering infrastructure, which was introduced in recent years. An AMI is the second generation of AMR system that has the demand response capability with control variables. This IP-based metering devices constantly transmit the measurement values to the customer billing centers. While this can improve the system reliability and power quality, the large expansion of devices requires a cost justification to meet complete 100% deployment which could take decades to meet the target. This transition from the current practise to the IP-based communication infrastructure may remain at slower

pace without governmental assistance. This setup can be costly in terms of maintenance as well as security aspects that can be subject to tampered by the malicious consumers. The drawbacks require multiple milestones of deployment by utilities who would be able to incentivize consumers and how to engage them into this data exchange with their repurposed mobile devices. This thesis has summarized the pros and cons of the costly deployment of AMI and suggested an economical alternative.

With the use of campus-wide metering testbed and the generous supports by the team from facilities management, it is believed that this work would largely impact the progress of technological exploration with alternatives that would be cost effective and sustainable. The current structure of AMI deployment is still in a fledging period although the initial deployment was commissioned on 10 campus buildings since January 2012. The accomplished infrastructure provides high percentage coverage of system observability, and the energy usage for those buildings fluctuate over time. The current AMI deployment has the coverage of up to 65 percent energy usages during the peak time.

Besides the IP-based “smart” meter deployment, there are 3 frequency disturbance recorders (FDR) have set up at each feeder for future research. This is a single-phase phasor measurement unit (PMU) that would be used to determine the system dynamics and stability for the study. Although this is not the main theme of this thesis, these advanced sensor units would enhance the observability of the campus

load monitoring.

The proposed method is designed to automatically extract data from images of electromechanical analog meters without real-time data observation ability. The proposed framework requires a wireless network environment and continuous power supply in the location of existing electromechanical meters, as well as Internet availability for real-time transmission to the cloud. The algorithm includes image segmentation, digital image processing, and matrix border grayscale detection analysis. The analysis in this algorithm is based on the four sub-dials rather than the whole plate surface. The algorithm will keep working when the sub-dials retain circle shapes without considering the shape, size, diameter, or configuration of the whole plate. The primary step in this algorithm is to binarize the original picture from colors to black and white only. The real-time data acquired from existing electromechanical meters will be fully implemented to improve the observability of the campus distribution grid without deploying expensive IP-based wired meters. These mobile devices which are connected through Wi-Fi to the cloud will provide real-time snapshots of operating states together with the other 10 on campus buildings that have IP-Based meters. The trending information from these devices will be compared in order to generate the common time-activity curves across all metered buildings. This may reveal energy data variation within a specific time period. Within a limited time-frame, the curve illustrates that the demanded quantity of energy consumption can be utilized to forecast or to adjust the system consumption as part of the study.

The simulation results show that the proposed method provides periodically extracted data to generate time-activity curves with other IP-based metering devices. The proposed application has been tested on one of the unmetered buildings which has reasonably large consumptions among those. Considering the situation that the mobile device could make an slight involuntary movement because of the gravity or vibration, additional circle recognition algorithms should be considered to compensate for camera position shift. Considerations to enumerate other types of analogy meters would include in the studies and adaptation of existing modules in meeting a manufacturer-specific requirement of their analog devices would be necessary. Although this approach is in the experimental stage, it offers an alternative to improve observability of the distribution network.

It is noted that there is still some future work that needs to be considered. There are a few significant error results generated by the data acquiring algorithm of the pointer analog meter. Setting a return value or false alarm if the current generated result is much larger or smaller than the previous value will decrease the number of significant errors, whereas the accuracy rating of these arranged images will be influenced slightly. In addition, we will try to correct the precision to 0.01, which means the reading accuracy will be percentile.

For the timer camera application algorithm, enhancement can be made to reconnect the server while experiencing sudden Wi-Fi network disconnection. Furthermore,

additional mobile devices would be deployed more in the future to study the load patterns of the campus that will be applied to other unmetered buildings. As image quantity may vary and in order to distinguish them, a threshold setting with different criteria can guarantee the accuracies of location tags and time-stamps for each taken photo image. For unmetered buildings with low reception of Wi-Fi availability, possible exploration of technologies, such as getting a cellular 4G Long-Term Evolution (LTE) device may be an option. For the completeness of putting the mobile devices for the rest of buildings, algorithms to extract different meter types will be investigated.

References

- [1] W. L. Sunshine, *Pros and Cons of Smart Meters*, 2014. [Online]. Available: <http://energy.about.com/od/metering/a/Pros-And-Cons-Of-Smart-Meters.htm>.
- [2] Y.Liu, *Frequency Disturbance Recorder(FDR) Installation Guide*, Power Information Technology(FNET) Lab, University of Tennessee, Knoxville., 511 Min Kao Building, Knoxville, US, Aug. 2012. [Online]. Available: <http://powerit.utk.edu/fdr/FDRInstallAndConfigGuide.pdf>.
- [3] Z. Xu and X. Li, “The construction of interconnected communication system among smart grid and a variety of networks,” in *Power and Energy Engineering Conference (APPEEC), Asia-Pacific*, Mar. 2010, pp. 1–5.
- [4] *AMR/AMI Infrastructure*, Digi International Inc, 2008. [Online]. Available: http://www.cstelectronics.co.za/Digi_AMI_and_AMR_whitepaper.pdf.
- [5] O.Pauzet, “The futere of smart metering:the case for public cellular communications,” *Metering International Issue*, vol. 3, pp. 38–39, 2011.

- [6] G. Deng, S. Fu, K. Shu, and J. Chen, "Discussion on advanced metering infrastructure," in *Proc. Electrical Measurement and Instrumentation*, vol. 47, no. 7A, Wuhan, China, Jun. 2010.
- [7] M. Music, A. Bosovic, N. Hasanspahic, S. Avdakovic, and E. Becirovic, "Integrated power quality monitoring system and the benefits of integrating smart meters," in *Compatibility and Power Electronics (CPE), 8th International Conference on*, Jun. 2013, pp. 86–91.
- [8] T. Baldwin, D. Kelle, J. Cordova, and N. Beneby, "Fault locating in distribution networks with the aid of advanced metering infrastructure," in *Proc. Power Systems Conference (PSC), Clemson University*, Mar. 2014, pp. 1–8.
- [9] T. Khalifa, K. Naik, and A. Nayak, "A survey of communication protocols for automatic meter reading applications," *IEEE Trans. Commun.*, vol. 13, no. 2, pp. 168–182, Feb. 2011.
- [10] R. S.Wang, H.Zhou and Z.Yi, "Concept and application of smart meter," *IEEE Trans. Power Syst.*, vol. 34, no. 4, Apr. 2010.
- [11] J.Roche, *AMR vs AMI*, PennWell Corporation, Oct. 2008. [Online]. Available: http://www.elp.com/articles/powergrid_international/print/volume-13/issue-10/features/amr-vs-ami.html.
- [12] M. Popa, "Smart meters reading through power line communications," *IEEE Trans. Inf. Theory*, vol. 2, no. 3, Aug. 2011.

- [13] *Modbus Protocol*, Trexon Inc., Jan. 2000. [Online]. Available: http://irtfweb.ifa.hawaii.edu/~smokey2/software/about/sixnet/modbus/modbus_protocol.pdf.
- [14] K. Swift, *Oncor Connects Advanced Metering Over Ethernet*, T&D World Magazine., Feb. 2003. [Online]. Available: <http://tdworld.com/smart-energy-consumer/oncor-connects-advanced-metering-over-ethernet>.
- [15] N. Massa, *Fiber Optic Telecommunication*, Springfield Technical Community College., 2000. [Online]. Available: <https://spie.org/Documents/Publications/20STEP20Module2008.pdf>.
- [16] V. Kalkunte, *Role of WiFi/IEEE 802.11n and Related Protocols in Smart Grid*, CTO, Datasat Technologies, 2010. [Online]. Available: http://www.comsocscv.org/docs/Workshop_092510_11nInSG.pdf.
- [17] M. LeMay and C. Gunter, “Cumulative attestation kernels for embedded systems,” *IEEE Trans. Smart Grid*, vol. 3, no. 2, pp. 744–760, Jun. 2012.
- [18] K. Balachandran, R. Olsen, and J. Pedersen, “Bandwidth analysis of smart meter network infrastructure,” in *Advanced Communication Technology (ICACT), 16th International Conference on*, Feb. 2014, pp. 928–933.
- [19] C. Brunschwiler, *Advanced Metering Infrastructure Architecture and Components*, Compass Security Blog, Feb. 2013. [Online]. Available: <http://blog.csnc.ch/2013/02/advanced-metering-infrastructure-architecture-and-components/>.

- [20] H. Saari, P. Koponen, E. Tahvanainen, and T. Lindholm, "Remote reading and data management system for kwh-meters with power quality monitoring," in *Metering and Tariffs for Energy Supply, Eighth International Conference on (Conf. Publ. No. 426)*, Jul. 1996, pp. 11–15.
- [21] D. Matheson, C. Jing, and F. Monforte, "Meter data management for the electricity market," in *Proc. Probabilistic Methods Applied to Power Systems, International Conference on*, Sep. 2004, pp. 118–122.
- [22] S.-H. Choi, S.-J. Kang, N.-J. Jung, and I.-K. Yang, "The design of outage management system utilizing meter information based on advanced metering infrastructure (AMI) system," in *Proc. IEEE 8th International Conference on Power Electronics and ECCE Asia (ICPE ECCE)*, May 2011, pp. 2955–2961.
- [23] J. Zhou, J. Hu, and Q. Yi, "Scalable distributed communication architectures to support advanced metering infrastructure in smart grid," *IEEE Trans. Parallel Distrib. Syst.*, vol. 23, no. 9, pp. 1632–1642, Sep. 2012.
- [24] *Advanced Metering Infrastructure and Customer Systems*, SmartGrid.gov, Feb. 2014. [Online]. Available: http://www.smartgrid.gov/recovery_act/deployment_status/ami_and_customer_systems.
- [25] *Smart Grid Industry Development Situation and Demand Analysis*, Shenzhen Hongda Technology Co. Ltd., Shenzhen, China, Aug. 2012. [Online]. Available: <http://www.hxdgroup.com/news/shownews.php?lang=cn&id=33>.

- [26] W. Luan, D. Sharp, and S. Lancashire, “Smart grid communication network capacity planning for power utilities,” in *Proc. Transmission and Distribution Conference and Exposition, IEEE-PES*, Apr. 2010, pp. 1–4.
- [27] C. Arrigoni, M. Bigoloni, I. Rochira, M. Rodolfi, F. Zanellini, C. Bovo, V. Merlo, G. Monfredini, M. Subasic, and R. Bonera, “Smart distribution system the ingrid project and the evolution of supervision & control systems for smart distribution system management,” in *Proc. AEIT Annual Conference*, Oct. 2013, pp. 1–6.
- [28] G. Casolino, A. Di Fazio, A. Losi, and M. Russo, “Smart modeling and tools for distribution system management and operation,” in *Proc. IEEE International Energy Conference and Exhibition (ENERGYCON)*, Sep. 2012, pp. 635–640.
- [29] H. H. Chen and C. Ma, “Strategic evaluation of energy and distribution management systems,” in *Proc. IEEE International Conference on Service Operations and Logistics, and Informatics. IEEE/SOLI*, Oct. 2008, pp. 641–646.
- [30] S. Depuru, L. Wang, V. Devabhaktuni, and N. Gudi, “Smart meters for power grid – challenges, issues, advantages and status,” in *Proc. Power Systems Conference and Exposition (PSCE), IEEE-PES*, Mar. 2011, pp. 1–7.
- [31] *AX Supervisor*, Tridium, Inc., 2011. [Online]. Available: http://www.tridium.com/galleries/datasheet_pdf/2011-T-AXS.FINAL.pdf.
- [32] J.-W. Cao, Y.-X. Wan, G.-Y. Tu, S.-Q. Zhang, A.-X. Xia, X.-F. Liu, Z. Chen, C. Lu, and Y.-D. Han, “Information system architecture for

- smart grids,” *Chinese Journal of Computers*, 2012. [Online]. Available: http://www.mit.edu/~caoj/pub/doc/jcao_j_sgsurvey.pdf.
- [33] S. Mohagheghi, J. Stoupiš, and Z. Wang, “Communication protocols and networks for power systems-current status and future trends,” in *Proc. IEEE/PES Power Systems Conference and Exposition*, Mar. 2009, pp. 1–9.
- [34] Z. Houidi and M. Meulle, “A new VPN routing approach for large scale networks,” in *Proc. 18th IEEE Intl. Conf. on Network Protocols (ICNP)*, Oct. 2010, pp. 124–133.
- [35] *Primary UD EPR Cable*, Aluminum or Copper Conductor. EPR Insulation. Bare Copper Concentric Neutrals. Low Density Polyethylene Jacket., One Southwire Drive Carrollton, GA, US, 2013. [Online]. Available: <http://www.southwire.com/ProductCatalog/XTEInterfaceServlet?contentKey=prodcatsheetEPR01>.
- [36] L. Zhang, Z. Yi, S. Wang, R. Yuan, H. Zhou, and Q. Yin, “Effects of advanced metering infrastructure (AMI) on relations of power supply and application in smart grid,” in *Proc. China International Conference on Electricity Distribution (CICED)*, Sep. 2010, pp. 1–5.
- [37] J. Wang and V.-C. Leung, “A survey of technical requirements and consumer application standards for IP-based smart grid ami network,” in *Proc. International Conference on Information Networking (ICOIN)*, Jan. 2011, pp. 114–119.

- [38] X. Yang, Y. Zhang, Q. Niu, X. Tao, and L. Wu, "A mobile-agent-based application model design of pervasive mobile devices," in *Proc. 2nd International Conference on Pervasive Computing and Applications*, Jul. 2007, pp. 1–6.
- [39] M. Shiraz, A. Gani, R. H. Khokhar, and E. Ahmed, "An extendable simulation framework for modeling application processing potentials of smart mobile devices for mobile cloud computing," in *Proc. 10th International Conference on Frontiers of Information Technology (FIT)*, Dec. 2012, pp. 331–336.
- [40] *Analog Electric Meter-Watthour Meter-Analog Only Electric Utility Meter*, ElectraHealth.com, 2014. [Online]. Available: http://www.stetzerizer-us.com/Analog-Electric-Meter--Watthour-Meter--Analog-Only-Electric-Utility_p-51.html.
- [41] *Advanced Metering Infrastructure (AMI)*, Electric Power Research Institution, Feb. 2007. [Online]. Available: <https://www.ferc.gov/EventCalendar/Files/20070423091846-EPRI-AdvancedMetering.pdf>.
- [42] *Advanced Metering Infrastructure (AMI) Cost/Benefit Analysis*, Electric Power Research Institution, Jun. 2012. [Online]. Available: <http://smartgridcc.org/wp-content/uploads/2012/08/Ameren-Ex.-3.1-AIC-AMI-Cost-Benefit-Analysis-Revised.pdf>.
- [43] V. Vesma, *Manual meter reading*, Jan. 2008. [Online]. Available: <http://www.vesma.com/tutorial/art-mmr.htm>.

- [44] C. King, *Advanced Metering Infrastructure (AMI) Overview of System Features and Capabilities*, eMeter Corporation, Sep. 2004. [Online]. Available: <http://sites.energetics.com/madri/toolbox/pdfs/background/king.pdf>.
- [45] *Advanced Metering Infrastructure*, Office of Electricity Delivery and Energy Reliability., Feb. 2008. [Online]. Available: http://www.netl.doe.gov/FileLibrary/research/energyefficiency/smartgrid/whitepapers/AMI-White-paper-final-021108--2--APPROVED_2008_02_12.pdf.
- [46] S. Depuru, L. Wang, and V. Devabhaktuni, "Support vector machine based data classification for detection of electricity theft," in *Proc. IEEE/PES Power Systems Conference and Exposition (PSCE)*, Mar. 2011, pp. 1–8.
- [47] M. Popa, "Data collecting from smart meters in an advanced metering infrastructure," in *Proc. 15th IEEE International Conference on Intelligent Engineering Systems (INES)*, Jun. 2011, pp. 137–142.
- [48] R. Berthier and W. Sanders, "Specification-based intrusion detection for advanced metering infrastructures," in *Proc. IEEE 17th Pacific Rim International Symposium on Dependable Computing (PRDC)*, Dec. 2011, pp. 184–193.
- [49] Y. Guo, C.-W. Ten, and P. Jirutitijaroen, "Online data validation for distribution operations against cybertampering," *IEEE Trans. Power Syst.*, vol. 29, no. 2, pp. 550–560, Mar. 2014.

- [50] Beckett.W., *Smart Mobile Device Security for the Enterprise*, AT&T Labs., Aug. 2010. [Online]. Available: <http://billwinkle.files.wordpress.com/2010/08/paper.pdf>.
- [51] T.-Y. Wu, W.-T. Lee, and C. F. Lin, "Cloud storage performance enhancement by real-time feedback control and de-duplication," in *Proc. Wireless Telecommunications Symposium (WTS)*, Apr. 2012, pp. 1–5.
- [52] L. Zheng, Y. Hu, and C. Yang, "Design and research on private cloud computing architecture to support smart grid," in *Proc. International Conference on Intelligent Human-Machine Systems and Cybernetics (IHMSC)*, Aug. 2011, pp. 159–161.
- [53] R. C. Gonzalez and R. E. Woods, *Digital Image Processing*, 2nd ed. Prentice-Hall, Inc., 2002.
- [54] S.-J. Zhang, *Image Engineering: Processing and Analysis*, 2nd ed. Qinghua University Press, Mar. 1999, vol. 1.
- [55] A. Liu and M. Gouda, "Firewall policy queries," *IEEE Transactions on, Parallel and Distributed Systems*, vol. 20, no. 6, pp. 766–777, Jun. 2009.
- [56] Huang, Y. Fang, S. Werner, J. Huang, N. Kashyap, and V. Gupta, "State estimation in electric power grids: Meeting new challenges presented by the requirements of the future grid," *IEEE Signal Process. Lett.* 29, no. 5, pp. 33–34, 2012.

- [57] *Xcode*, Apple Inc., Jan. 2014. [Online]. Available: <http://developer.apple.com/xcode/downloads>.
- [58] Q. Zhang and Z. Wang, *Proficient in Matlab image processing*, 2nd ed. Electronic Industry Press, Apr. 2012.

Appendix A

STATISTICAL RESULTS

Power and Energy Measurement Datasets for the Ten Metered Buildings

This section provides the historical statistics of the metering information of power and energy measurements from campus AMI system.

1. Figure A.1 shows results of the Building 19, which is the Chemical Sciences and Engineering building. The top figure illustrates the time-activity curves of the energy values in this building. The energy consuming is a cumulative procedure, which means, after a time duration, the newly presented value must

be equal to the original value plus the energy consumption of this time interval. This is the reason that the energy values are incremental. According to the time-activity curve of energy values, we observed there are two circuits in the Chemical Sciences and Engineering building, which are 208-V and 480-V, separately. The circuit with 208-V is primarily responsible for consumption limited electrical appliances, e.g., light and power outlets, while the circuit with 480-V is in charge of large electric facilities such as air conditioning and laboratory equipment. The green line demonstrates the total consumption of this building, which is the sum of two circuits. It should be mentioned that the black bars in the figures represent different quarters of a year.

Unlike energy values, power values illustrate the specific amounts of power usages for different time durations. The visualization result of the power value is fluctuant because the electricity consumption in different time-frames is unfixed. In addition, in the measurements of energy and power, if a fault appeared, the corresponding return value in a time-stamp with a fault occurred is 0. Then, we observed that the energy values of Building 19 are completely correct, while there are four or five faults that happened in power measurement during the whole time period.

2. Figure A.2 shows the results of Building 31, which is the Douglass Houghton Hall (DHH). There is only one circuit in this building; we observed that the overall trend is correct even though a couple of faults occurred. We can still consider

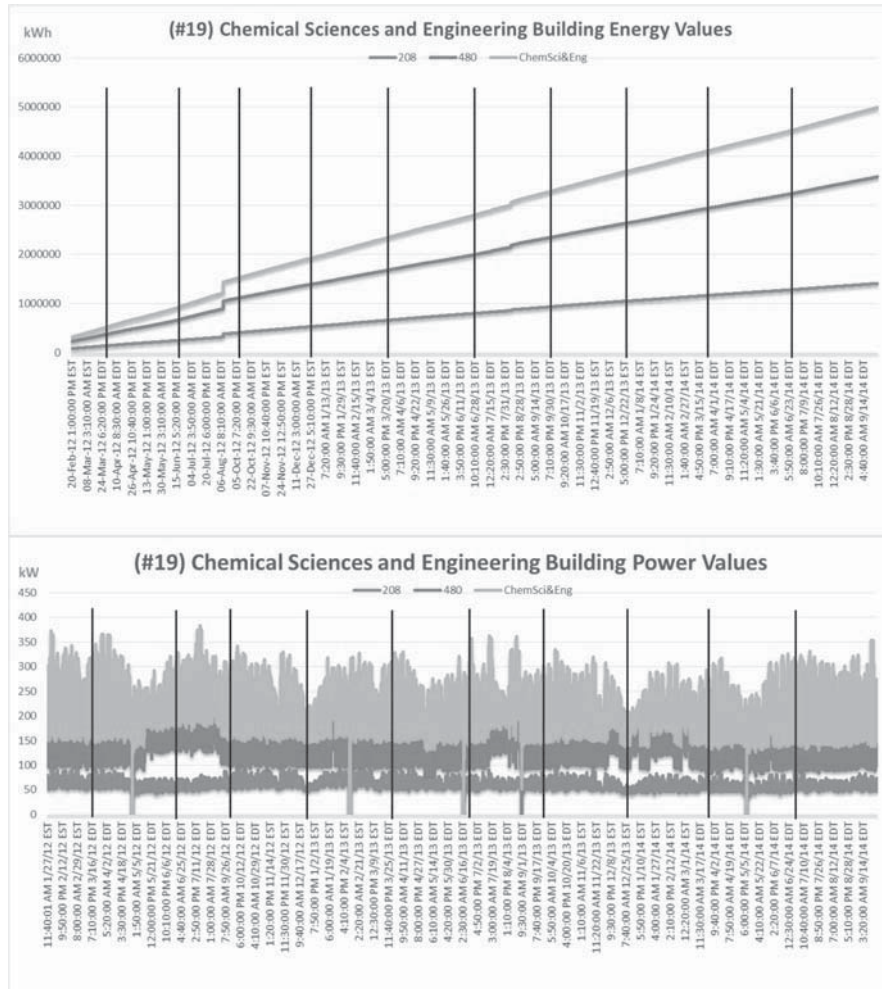


Figure A.1: (19) Chemical Sciences and Engineering Building.

the energy measurement function in this system is under normal operation. About the power values, there are three significant reductions in the time-activity curve. Checking the timelines for these three abnormal conditions, we observed all of these three durations covers the time duration from the beginning of May to the end of August, which is the summer vacation in Michigan Tech. Furthermore, DHH is a student dormitory, where most of the students living here will be back home during this time period. From this, the historical archive

result of power values in this building could be interpreted.

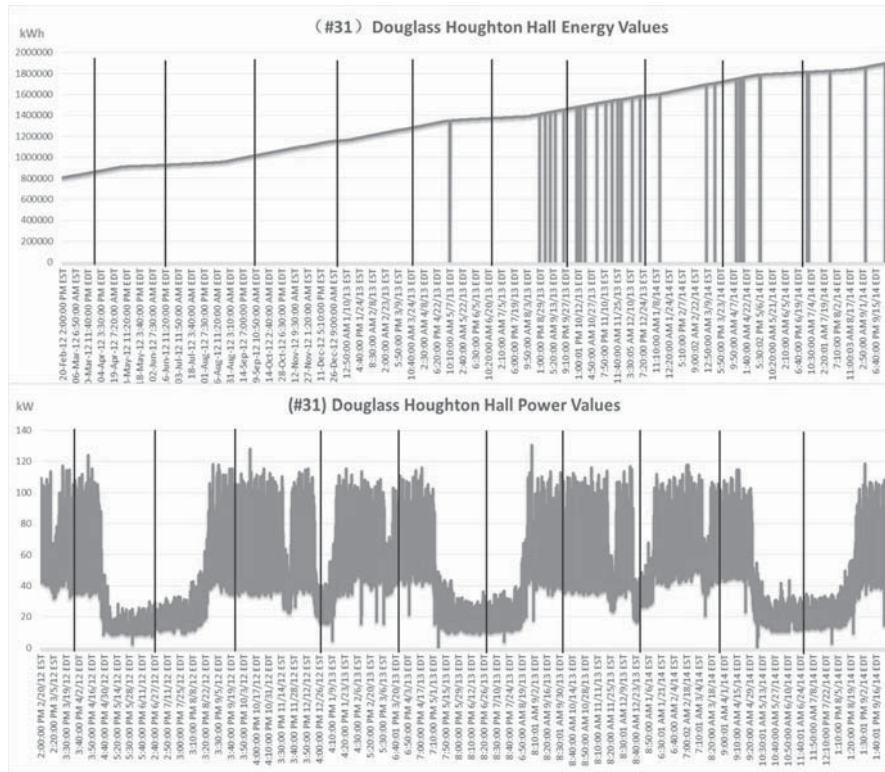


Figure A.2: (31) Douglass Houghton Hall (DHH).

3. Figure A.3 shows the energy and power values of the Building 17, which is the J. R. Van Pelt and Opie Library. Similar with DHH, there is only one circuit in library. Also, there are few faults in energy values but they do not affect the overall cumulative trend. Because the library should provide a 24 hour academic environment for students, there is an uninterrupted power supply under normal circumstances. That is the reason that there are no obvious decreases during the whole time period.
4. Figure A.4 shows the data results of McNair Hall, which is a student residence

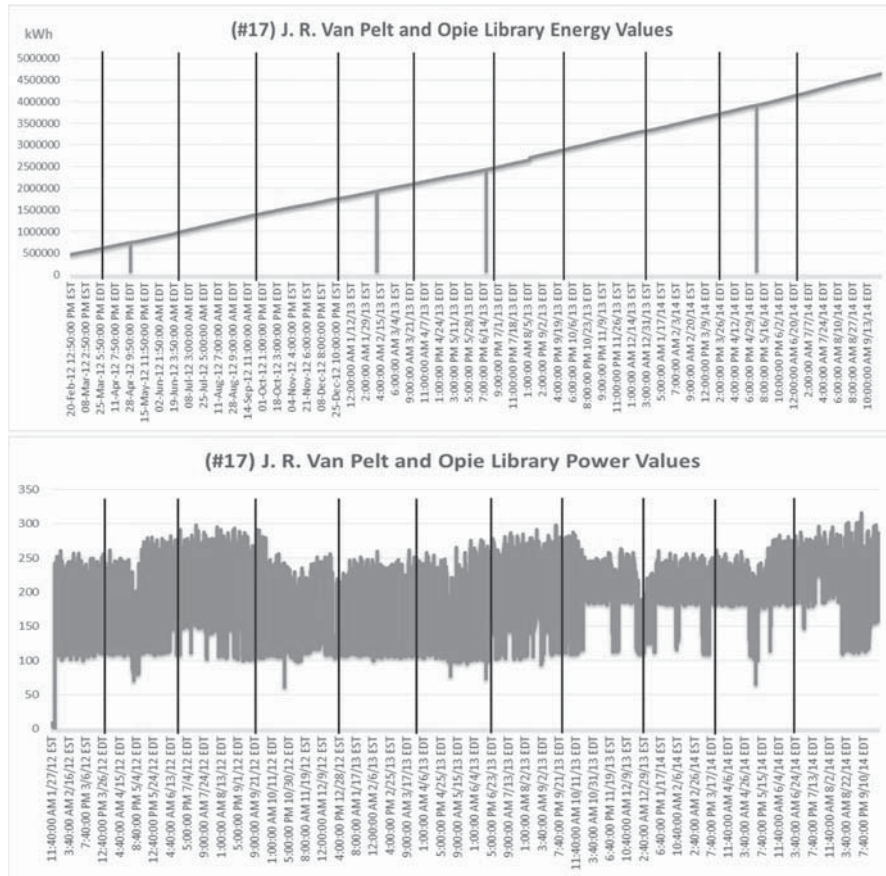


Figure A.3: (17) J. R. Van Pelt and Opie Library.

hall. As shown in the results, there are two circuits in this building, which are responsible for controlling and monitoring the power supply of east and west living quarters, separately. According to the energy result, we observed the energy consumption of the west section of McNair Building is higher than the east. In addition, the McNair west circuit has a perfect rise curve, while there are some faults that existed in the rise of energy values in east McNair. Similar with the power results in DHH, there are three obvious decreases in the power time-activity curves of McNair Hall. Both of the energy and power measuring functions in McNair Hall could be considered as normal.

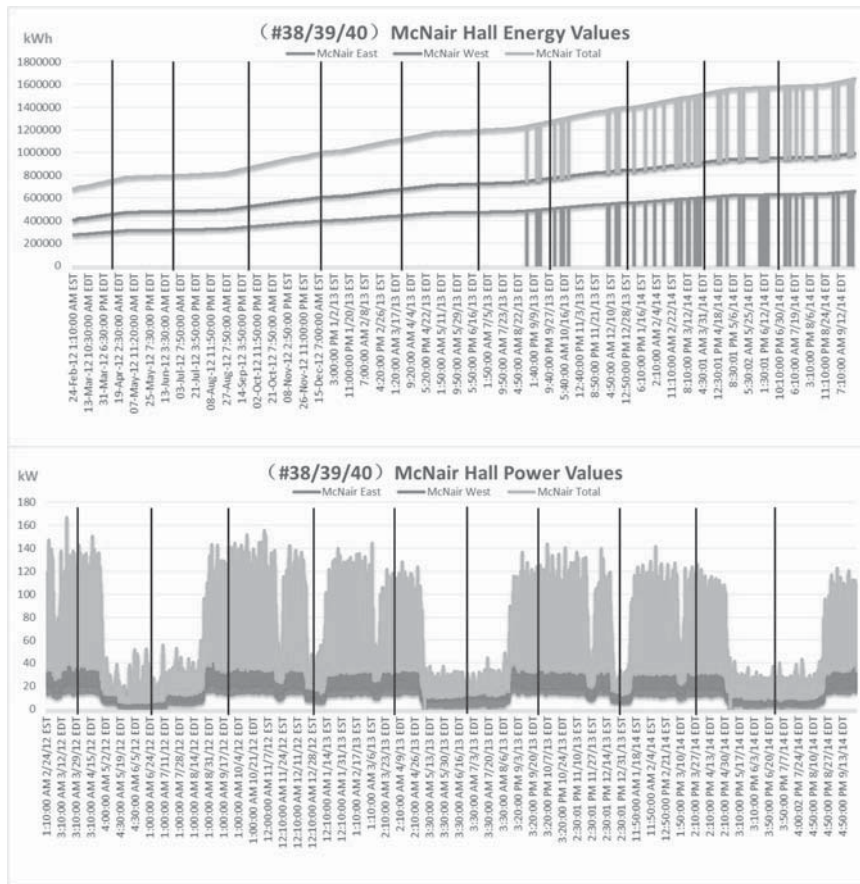


Figure A.4: (38/39/40) McNair Hall.

- Figure A.5 shows the results of Building 7, which is the Electrical Energy Research Center (EERC). There are three circuits that can be seen in the data results of EERC, which are named as SUB1, SUB2, and SUB3, separately. The SUB1 circuit is responsible for the power supply of the main building and large electrical appliances. That is why it has more energy consumption than the other two circuits. Comparing with previous results, we could affirm that, both of the energy and power measurement functions in this building are running correctly. There is one FDR unit in this building.

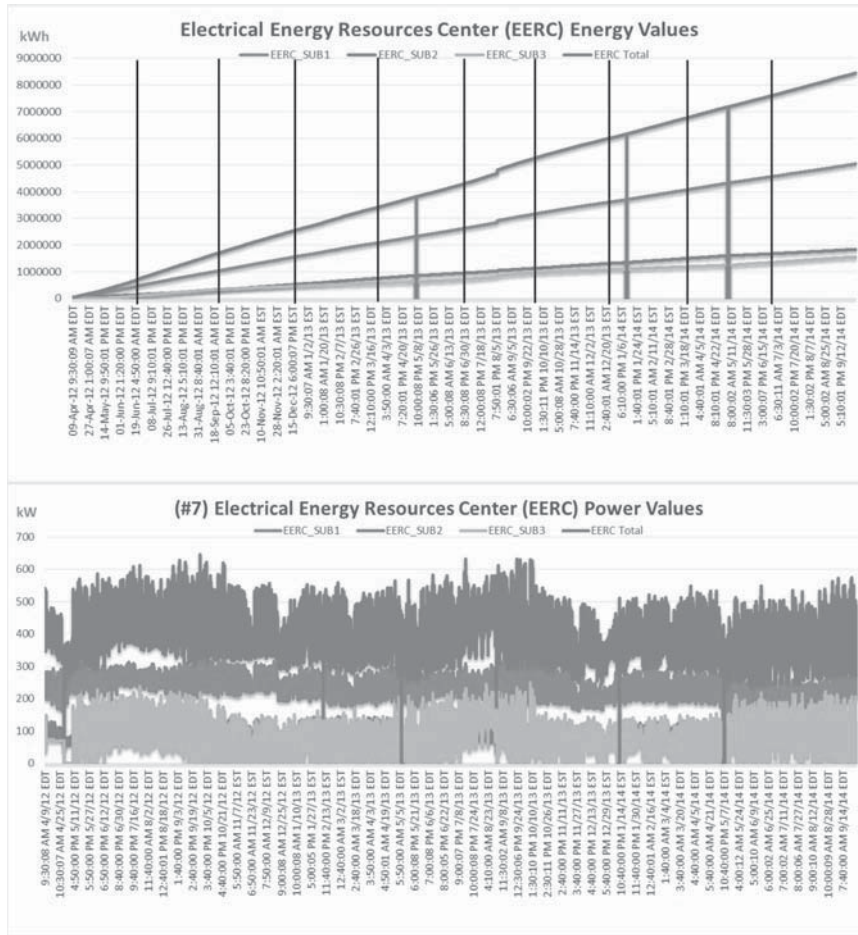


Figure A.5: (7) Electrical Energy Research Center (EERC).

6. Figure A.6 shows the results of Building 24, which is the Student Development Complex (SDC). This building is the gymnasium at Michigan Tech. Because the constant refrigeration and illumination in the ice arena need to consume large amounts of electric power, there is a designated circuit to guarantee the power supply. The circuit named TA is responsible for the main building, which contains the basketball courts, fitness center, swimming pool, and the other facilities. The TB circuit is in charge of the power consumption of outdoor

venues, which contains the football field and parking lots. Also, both of the time-activity curves of energy and power values are shown appropriately. Another FDR device is installed in this building.

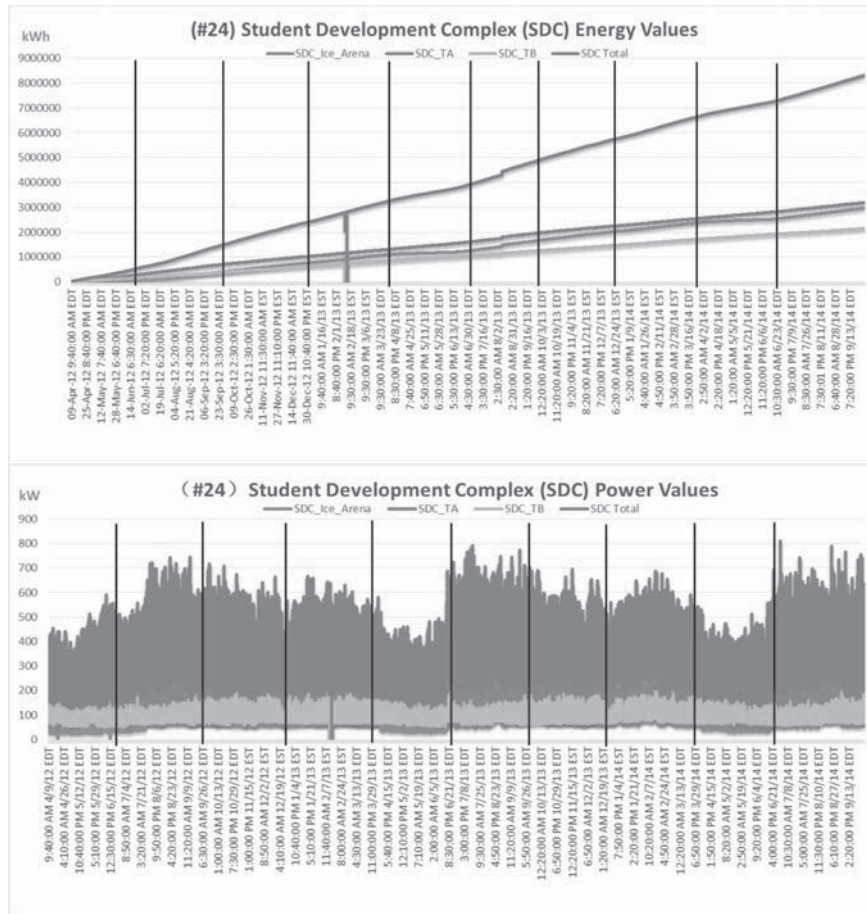


Figure A.6: (24) Student Development Complex (SDC).

7. Figure A.7 shows the statistical results of Building 12, which is the Minerals and Materials Engineering (M&M) building. Comparing with the data results of the Chemical Science and Engineering building, we can infer that the energy values of these two circuits are normal. However, the time-activity curve of power values is unusual as we can not observe the values of circuit 208-V from

the end of June 2013 until now. Different than with the system fault response, the fault that appears here can be inferred as disconnecting, because the data storage interface of this building is blank rather than full of zeros.

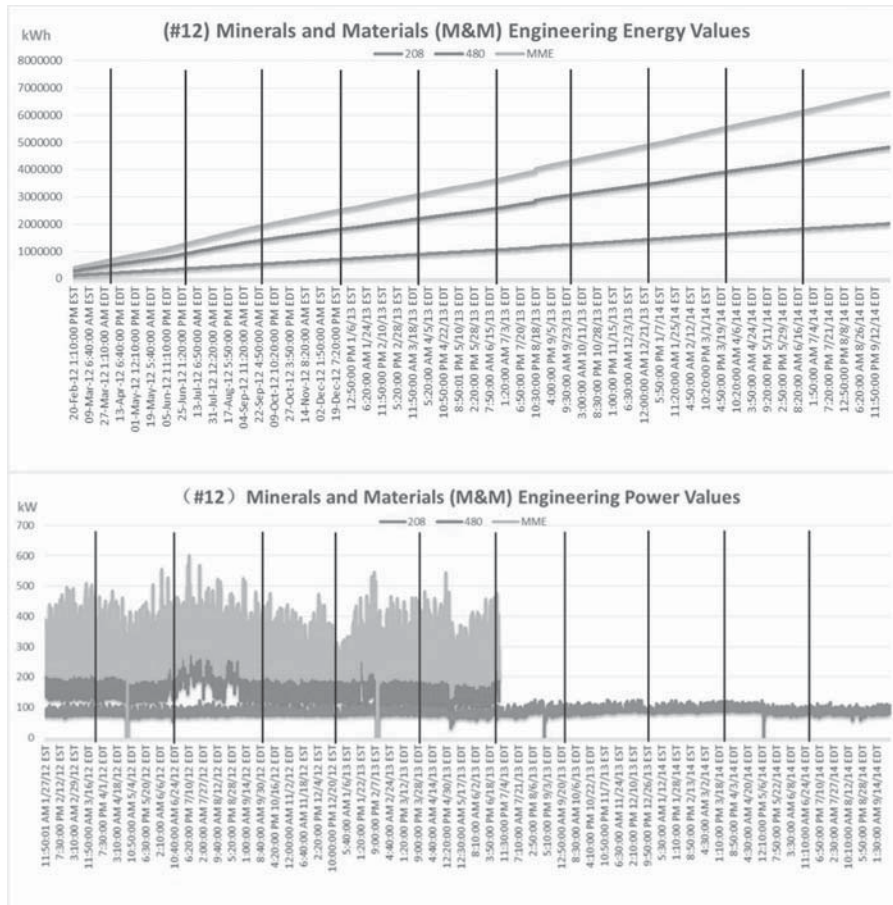


Figure A.7: (12) Minerals and Materials Engineering (M&M).

- Figure A.8 shows the results of Building 8, which is the Dow Environmental Science and Engineering building. Because numerous zeros existed in the historical dataset of this building, which could be treated as the fault return values in the data list, the values of the data fluctuated strongly during the past time period. This is also the reason why the energy result seems like a bar chart rather than

a rising curve. Regarding the power result, we found the time-activity curve is similar to the result of M&M building, but the data results in the data sheet are quite different. The power values in this building from the beginning of February 2013 until now are zeros. Both of the abnormal data results indicate the measurement functions in this building are damaged.



Figure A.8: (8) Dow Environmental Science and Engineering Building.

9. Figure A.9 shows the results of Building 18, which is the U. J. Noblet Forestry and Wood Products building. Similar with the energy data result of the Dow building, the energy cumulative curve in this building also seems like a bar

chart and the results of the two circuits are covered by the total result. According to the energy data list, we observed the reason for this is the same as the Dow building as to why many zeros existed. Comparing with the previous results of power, we can infer that the power result here is under a normal condition.

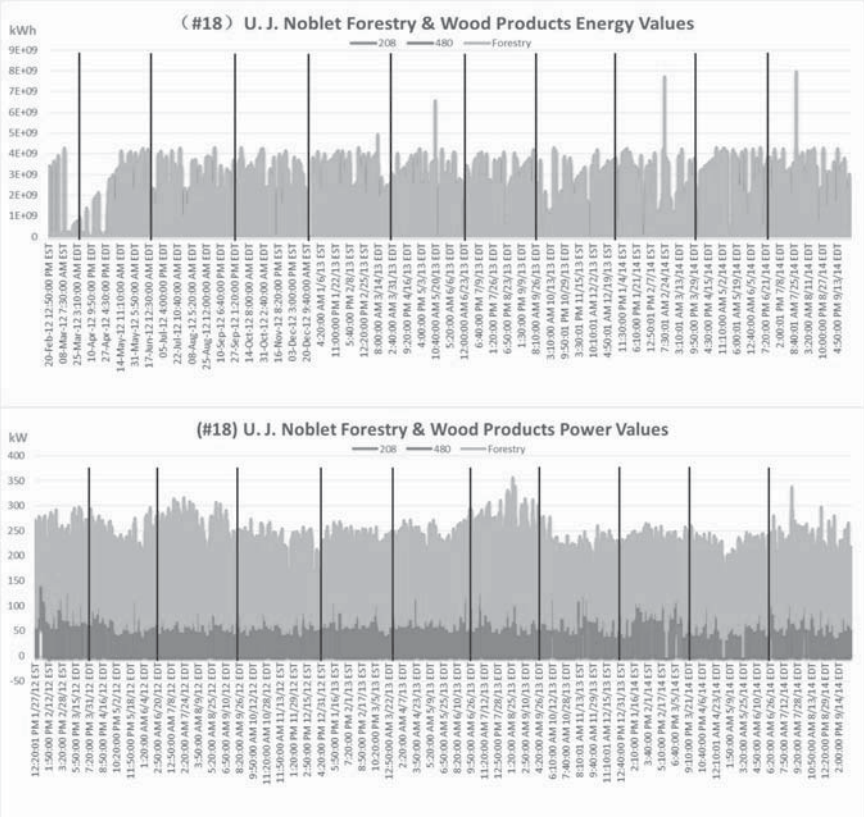


Figure A.9: (18) U. J. Noblet Forestry and Wood Products Building.

- Figure A.10 shows the data time-activity curves of the energy and power values of Building 37. Building 37 is Wadsworth Hall, which is also a student residence hall. Comparing with the previous results of power values, we observed the power result is in normal working state, even though the summer vacation

decreases are not distinct enough. The energy result in Wadsworth Hall is interesting. The overall time-activity curve consists of several small cumulative curves. According to the energy data list, the energy measurement function in this building always restarts after an unfixed time duration. One reason for this operation can be inferred that the growth rate of energy values is too fast because the slope of each sub-curve is higher than the previous rising curves.

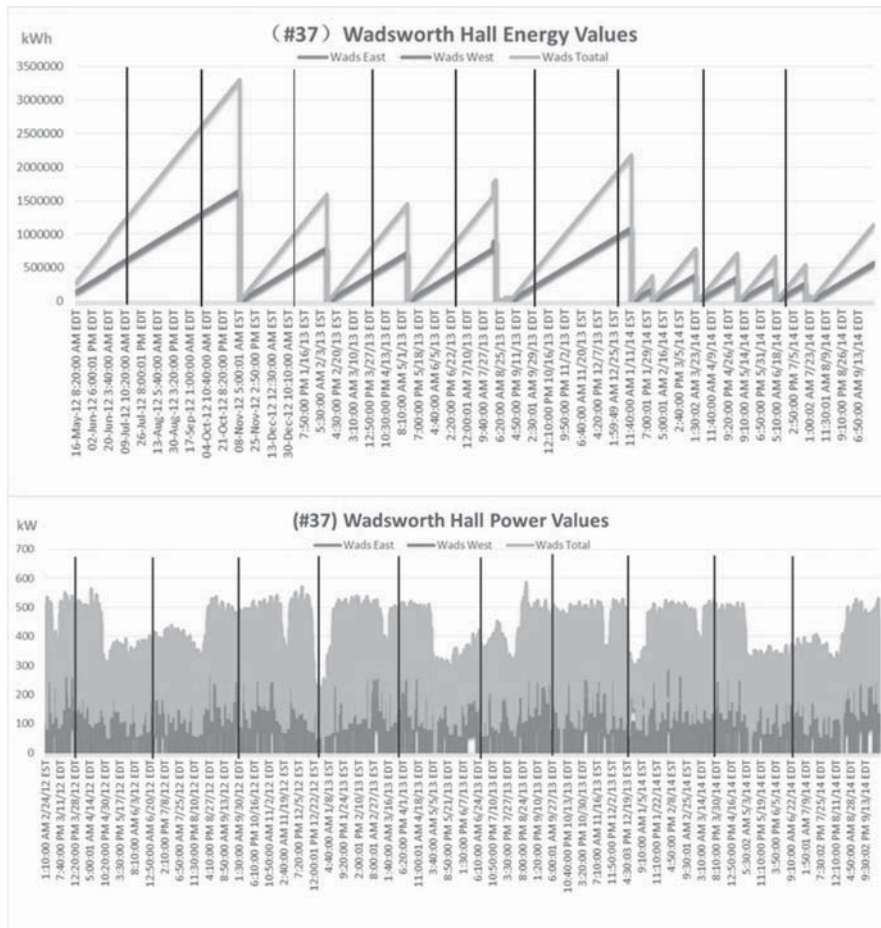


Figure A.10: (37) Wadsworth Hall.